and benzo[*a*]pyrene. Additionally, it remains undetermined whether TCDD, an environmental pollutant, influences IgE production in B cells, although a couple of reports have described that TCDD enhances IgE synthesis in B cells (6, 7).

The aryl hydrocarbon receptor (AhR) is a transcriptional factor possessing basic helix-loop-helix/Per-aryl hydrocarbon receptor nuclear translocator (Arnt)-Sim motif, which binds to various kinds of xenobiotics, including TCDD (8, 9). Upon binding to the ligand, AhR translocates to the nuclei, followed by formation of the heterodimeric complex with Arnt. The AhR–Arnt complex induces expression of a number of monooxygenase genes such as cytochrome P4501A1 (*CYP1A1*), *CYP1A2* and *CYP1B1*, by binding to the xenobiotic responsive element on the target genes, playing a key role in metabolism of xenobiotics (8, 9). In addition, it has been recently reported that AhR directly affects cell cycle regulation in response to an agonist, although it is controversial whether it can inhibit or promote proliferation (10), and that AhR directly interacts with nuclear factor κB, down-regulating its biological activities (11).

To explore the activity of IL-4 and IL-13 on B cells, we employed a microarray analysis, and it turned out that the *AHR* gene was included in the identified genes. In this article, we characterize the induction and activation mechanism of AhR by IL-4 in B cells. These results suggest that induction and activation of AhR are novel biological activities of IL-4 and IL-13 on B cells and that consequently IL-4 and IL-13 should be involved in the metabolism of xenobiotics by induced and activated AhR in B cells. In contrast, TCDD did not affect IgE production or CD23 expression by IL-4 in B cells, denying the synergistic effect of TCDD on IgE production by IL-4.

Methods

Reagents

Cycloheximide, TCDD and MG132 were purchased from Sigma–Aldrich (St Louis, MO, USA), Wako (Osaka, Japan) and Calbiochem (San Diego, CA, USA), respectively.

Cells

DND-39 cells and HepG2 cells were maintained in RPMI 1640 medium or Dulbecco's modified Eagle's medium supplemented with 10% FCS, 100 μg ml $^{-1}$ streptomycin and 100 U ml $^{-1}$ penicillin. IL-13Rα1-transfected DND-39 cells were prepared and maintained as described before (12). PBMCs were separated from healthy human volunteers using Lymphoprep™ (Axis-Shield, Oslo, Norway), and then B cells were isolated using Dynabeads™ M-450 CD19 (Dynal, Oslo, Norway), and cultured in the same way as DND-39 cells. DND-39 cells, HepG2 cells and human B cells were stimulated with 10 ng ml $^{-1}$ of IL-4 (Peprotech, Rocky Hill, NJ, USA) and/or 10 μg ml $^{-1}$ of anti-IgM antibody (Cappel, Aurora, OH, USA) and/or 0.5 μg ml $^{-1}$ of anti-CD40 antibody (Immunotech, Marseille, France) for the indicated times. Mouse B cells were isolated from spleen cells using StemSep™ B cell enrichment (StemCell Technologies Inc., Vancouver, Canada) and maintained in RPMI 1640 medium supplemented with 10% FCS, 50 μM 2-mercaptoethanol, 100 μg ml $^{-1}$ streptomycin and 100 U ml $^{-1}$ penicillin. Mouse B cells were stimulated with 10 ng ml $^{-1}$ of IL-4 (Chemicon International, Temecula, CA, USA) and/or 20 μg ml $^{-1}$ of LPS (Sigma–Aldrich).

Microarray analysis

Procedures of probe preparation and microarray analysis were performed as described before (13). The microarray analyses of complementary RNA from IL-13Rα1-transfected DND-39 cells were performed with human high-density oligonucleotide probe arrays (HG-U95Av2 Array) representing ~10 000 full-length, non-redundant genes supplied by Affymetrix. Hybridized probe arrays were read using a Hewlett-Packard GeneArray scanner (HP2500A, Hewlett-Packard, Palo Alto, CA, USA). The data were analyzed using Gene Chip software, Suite ver.4.0 (Affymetrix). Integrity of the RNA was verified before reverse transcription (RT) by visualization of the 28S and 18S ribosomal RNA bands on an agarose gel. Hybridization quality was checked by measuring the ratio of hybridization intensities of the 3′–5′ regions of control genes.

RT–PCR

Total RNA was extracted by ISOGEN (Nippongene, Tokyo, Japan). The RT reaction primed with random hexamer was performed using GeneAmp RNA PCR Kit (Applied Biosystems Japan, Tokyo, Japan). The PCR reaction was performed with cDNA as a template using the indicated primers after an initial 1-min denaturation at 96 C, followed by the indicated cycles of 96 C for 1 min, the indicated annealing temperature for 1 min and 72 C for 1 min. The cycles used were 34, 31, 21, 32, 20 and 25, for human AhR, human Arnt, human GAPDH, the hemagglutinin-tagged truncated form of STAT6 (HA-STAT6DN), human β-actin and the human germline ε transcript, respectively. The annealing temperatures used were 58, 58, 54, 58, 62 and 55 C for AhR, Arnt, GAPDH, HA-STAT6DN, β-actin and the germline ε transcript, respectively. The PCR primers used were 5′-AGTCTGTTATAACCCAGAC-CAG-3′, and 5′-GCATCACAACCAATAGGTGTGA-3′ for AhR; 5′-GATGCAGGAATGGACTTGGCT-3′, and 5′-CTTTCCTAAG-AGTTCCTGTGGCT-3′ for Arnt; 5′-GAAGGTGAAGGTCGGA-GT-3′ and 5′-GAAGATGGTGATGGGATTTC-3′ for GAPDH; 5′-CTAGCATGTATCCTTATGATGTTCCTGATTATGCTGGTAC-3′ and 5′-CCTCAGCCCCCTTCTGCA-3′ for HA-STAT6DN; 5′-TCACCCACACTGTGCCCATCTACGA-3′ and 5′-CAGCG-GAACCGCTCATTGCCAATGG-3′ for β-actin and 5′-CTGGGAG-CTGTCCAGGAACC-3′ and 5′-GCAGCAGCGGGTCAAGG-3′ for the germline ε transcript, respectively.

Immunoprecipitation and western blotting

Procedures of immunoprecipitation and western blotting were carried out as previously described (14). The samples were applied to SDS-PAGE and then electrophoretically transferred to polyvinylidene difluoride membranes (Amersham Biosciences, Buckinghamshire, UK). The antibodies used for immunoprecipitation and western blotting were anti-AhR antibody (Santa Cruz Biotechnology, Santa Cruz, CA, USA), anti-Arnt antibody (Santa Cruz Biotechnology), anti-actin antibody (Biomedical Technologies, Stoughton, MA, USA) and anti-histone deacetylase class 1 (HDAC1) antibody (Santa Cruz Biotechnology). The proteins were visualized by enhanced

chemiluminescence (Amersham Biosciences). Fractionation of cell lysates was performed using NE-PER (Pierce Chemical Co., Rockford, IL, USA).

Mice

C57/BL6 and Balb/c mice were purchased from CLEA Japan, Inc. (Tokyo, Japan). STAT6-deficient mice and AhR-deficient mice were prepared as described before (15, 16). All experiments were approved by the Saga University Animal Care and Use Committee.

Generation of DND-39 cells expressing the truncated form of STAT6

The plasmid encoding STAT6DN was prepared as previously described (17). This plasmid was transfected into DND-39 cells by electroporation, and the transfectants were maintained with a medium containing 2.5 mg ml $^{-1}$ of Geneticin (Sigma–Aldrich).

Real-time PCR analysis

Quantitative analysis of mRNA expression was performed using the ABI PRISM™ 7000 sequence detection system (Perkin-Elmer Japan, Urayasu, Japan), as described before (13). To calculate the copy numbers for each gene, standard curves were generated using a plasmid encoding that gene whose copy numbers were known. The PCR primers used were 5′-AACCAGTGGCAGATCAACCAT-3′ and 5′-CCCATGCCAAAGATAATCACC-3′ for human CYP1A1; 5′-CACTCTCTTTGGTTTGGGCA-3′ and 5′-CTCCCCTGGAGACACCTTAAA-3′ for mouse CYP1A1; 5′-TCACCCACACTGTGCCCATCTACGA-3′ and 5′-CAGCGGAACCGCTCATTGCCAATGG-3′ for human β-actin; 5′-ACTATTGGCAACGAGCGGTTC-3′, and 5′-GGATGCCACAGGATTCCATACC-3′ for mouse β-actin; 5′-CAATACTTCCACCTCAGTTGGC-3′, and 5′-GCATCACAACCAATAGGTGTGA-3′ for human AhR and 5′-GAAGGTGAAGGTCGGAGT-3′, and 5′-GAAGATGGTGATGGGATTTC-3′ for human GAPDH, respectively. The TaqMan™ probes used were 5′-CCCTGATGGTGCTATCGACAAGGTGT-3′ for human CYP1A1, 5′-AAAGTGCATCGGAGAGACCATTGGC-3′ for mouse CYP1A1, 5′-ATGCCCTCCCCCATGCCATCCTGCGT-3′ for human β-actin, 5′-CCTGAGGCTCTTTTCCAGCCTTCCTTCT-3′ for mouse β-actin, 5′-AGCCACCATCCATACTTGAAATCCGG-3′ for human AhR and 5′-CAAGCTTCCCGTTCTCAGCC-3′ for human GAPDH, respectively.

ELISA for IgE

Mouse spleen cells were maintained in RPMI 1640 medium supplemented with 10% FCS (HyClone, South Logan, UT, USA), 1 mM sodium pyruvate (Invitrogen Corp., Carlsbad, CA, USA), 10 mM HEPES (pH 7.4), 0.1 mM non-essential amino acids (GIBCO BRL), 50 μM 2-ME, 100 μg ml $^{-1}$ streptomycin and 100 U ml $^{-1}$ penicillin, and incubated with 1 ng ml $^{-1}$ of IL-4 and 0.5 μg ml $^{-1}$ of anti-CD40 antibody (BD Biosciences, San Jose, CA, USA) in the presence of the indicated concentrations of TCDD for 5 days. ELISA for mouse IgE was performed using a mouse IgE ELISA Quantitation kit (Bethyl, Montgomery, TX, USA).

Flow cytometry for CD23

Flow cytometric analysis of CD23 on spleen cells was performed using FITC-labeled anti-B220 antibody (BD Biosciences) and PE-labeled CD23 antibody (BD Biosciences). Quantitation of the surface staining was performed using FACSCalibur, and data were analyzed using Cell Quest software (BD Biosciences).

Results

Identification of IL-4- and IL-13-inducible genes in a human Burkitt lymphoma cell line, DND-39

To identify the biological activity of IL-4 and IL-13 on B cells, we used a microarray analysis. The microarray experiments were designed based on the guidelines of Minimum Information About a Microarray Experiment. To exclude the complexity related to the heterogeneity of primary human B cells, we used a human Burkitt lymphoma cell line, DND-39. Then the samples were prepared from DND-39 cells expressing IL-13Rα1 stimulated with either IL-4 or IL-13 for either 24 or 48 h. Of the 10 000 annotated genes present on the arrays, IL-4 and IL-13 augmented expression of 22 and 16 genes at 24 h, respectively, and 14 and 45 genes at 48 h, respectively. Among these genes, 11 genes at 24 h and 13 genes at 48 h were commonly up-regulated by both IL-4 and IL-13. The findings that the *IGHE* gene coding for the Ig ε H chain constant region and the *FCER2* gene coding for CD23 were included in the overlapped genes proved the appropriateness of this microarray analysis; it is well known that IL-4 or IL-13 induces expression of these genes (18, 19). The *AHR* gene was consistently induced by both IL-4 and IL-13 at both 24 h (8.9-fold and 7.0-fold, respectively) and 48 h (5.1-fold and 5.0-fold, respectively), raising the possibility that the *AHR* gene is a novel IL-4- or IL-13-inducible gene in B cells (data not shown).

Induction of AhR by IL-4 in DND-39 cells and human and mouse primary B cells

To validate further the result that induction of AhR was up-regulated by IL-4 or IL-13 in the microarray analysis, we analyzed expression of AhR induced by IL-4 by RT–PCR. Upon stimulation of IL-4, AhR started to be induced and reached a peak at 3 h in DND-39 cells, and then declined (Fig. 1A). In contrast, another component of the complex, Arnt, was not affected by IL-4. To address whether the induction of AhR by IL-4 in DND-39 cells required *de novo* protein synthesis, we next analyzed the effect of cycloheximide on the induction. The induction of AhR by IL-4 was not affected up to 50 μg ml $^{-1}$ of cycloheximide (Fig. 1B). These results suggested that induction of AhR by IL-4 probably did not require *de novo* protein synthesis.

To address whether IL-4 up-regulates AhR production at not only the mRNA level but also the protein level, we next analyzed AhR induction by IL-4 using western blotting. IL-4 induced protein synthesis of AhR in DND-39 cells, whereas HepG2 cells constitutively expressed AhR and IL-4 did not affect the induction (Fig. 1C). Mouse spleen B cells derived from Balb/c or C57/BL6 strains also showed that IL-4 alone could enhance

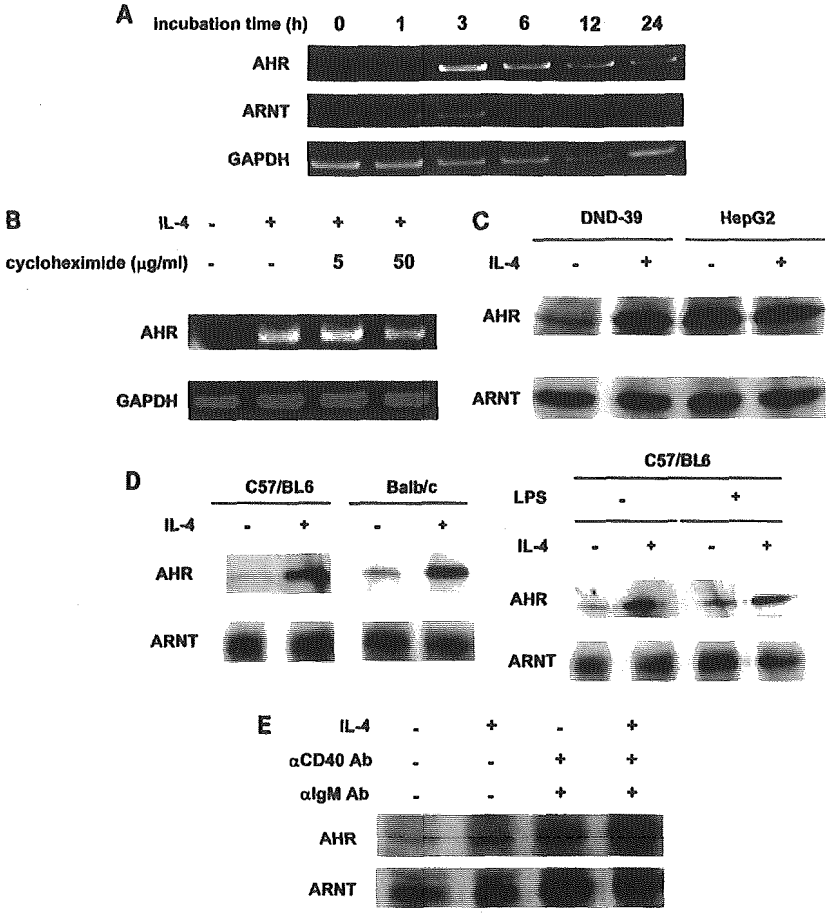

Fig. 1. Induction of AhR in B cells. (A) Total RNA was extracted from DND-39 cells stimulated with 10 ng ml $^{-1}$ of IL-4 for the indicated times, and then RT-PCR for AhR, Arnt and GAPDH was performed. (B) Total RNA was extracted from DND-39 cells stimulated with 10 ng ml $^{-1}$ of IL-4 for 6 h. The indicated concentrations of cycloheximide were added 30 min before the addition of IL-4. Then RT-PCR for AhR and GAPDH was performed. (C) Cell lysates were prepared from DND-39 cells and HepG2 cells stimulated with 10 ng ml $^{-1}$ of IL-4 for 24 h, and then western blotting was performed using either anti-AhR antibody or anti-Arnt antibody. (D) Immunoprecipitates with either anti-AhR antibody or anti-Arnt antibody were prepared from spleen B cells derived from C57/BL6 or Balb/c strains stimulated with 10 ng ml $^{-1}$ of IL-4 and/or 20 μg ml $^{-1}$ of LPS for 24 h, and then western blotting was performed using either anti-AhR antibody or anti-Arnt antibody. (E) Cell lysates were prepared from human primary B cells stimulated with 10 ng ml $^{-1}$ of IL-4 and/or 10 μg ml $^{-1}$ of anti-IgM antibody and/or 0.5 μg ml $^{-1}$ of anti-CD40 antibody for 24 h, and then western blotting was performed using either anti-AhR antibody or anti-Arnt antibody.

AhR production (Fig. 1D). LPS, which had been reported to induce AhR (20), had little effect on AhR induction. Expression of Arnt was unchanged by the stimulation. In human peripheral B cells, IL-4 alone only slightly induced AhR, whereas co-stimulants of anti-IgM antibody and anti-CD40 antibody significantly augmented the induction (Fig. 1E). Although expression of Arnt was augmented by co-stimulants of anti-IgM antibody and anti-CD40 antibody, IL-4 had no effect on the induction. We confirmed that the same amounts of proteins were loaded in each lane by Coomassie blue staining (data not shown). These results demonstrated that IL-4 had the ability to induce AhR in B cells, probably without *de novo* protein synthesis, although the co-stimuli to maximize the AhR expression were different in mouse and human B cells.

STAT6 dependency of AhR induction by IL-4

It is well known that a transcription factor, STAT6, plays critical roles for biological activities of IL-4 and IL-13 (21, 22). We next investigated whether AhR induction by IL-4 in B cells is dependent on STAT6. For this purpose, we first generated DND-39 cells expressing a truncated form of STAT6. This form lacked the SH2 domain and the activating domain for transcription; we had already shown that it acted as a dominant negative form of STAT6 (17). We used two independent clones expressing the truncated form. We confirmed that induction of the germline ε transcript by IL-4 was diminished in these transfectants (Fig. 2A). When these transfectants were stimulated with IL-4, AhR was not induced, whereas induction of AhR was detected in parental cells and mock-transfected

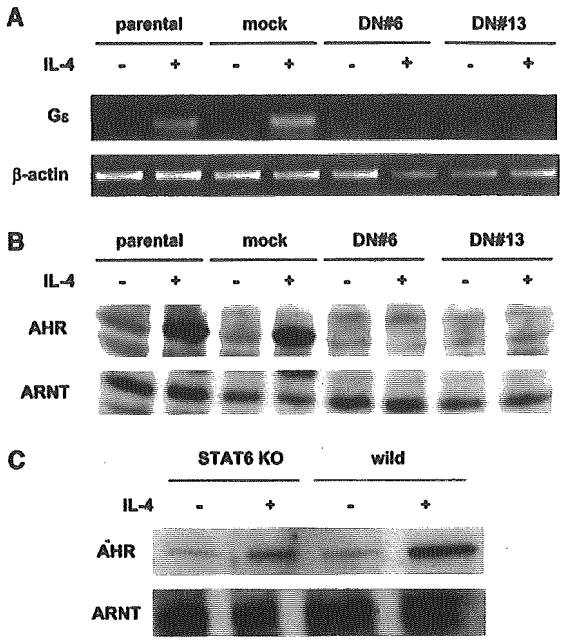

Fig. 2. Dependency of STAT6 of AhR induction in B cells. Total RNA (A) or cell lysates (B) were prepared from parental DND-39 cells, mock-transfected DND-39 cells and STAT6DN (#6 and #13) stimulated with 10 ng ml $^{-1}$ of IL-4 for 24 h. Then RT-PCR for the germline ε transcript or β-actin (A) or western blotting using either anti-AhR antibody or anti-Arnt antibody (B) was performed. (C) Immunoprecipitates with either anti-AhR antibody or anti-Arnt antibody were prepared from spleen B cells derived from wild mice or STAT6-deficient mice of C57/BL6 strain stimulated with 10 ng ml $^{-1}$ of IL-4 for 24 h, and then western blotting was performed using either anti-AhR antibody or anti-Arnt antibody.

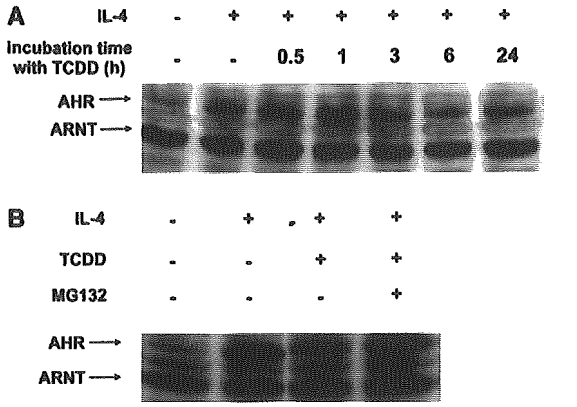

Fig. 3. Degradation of AhR proteins by TCDD. (A) Cell lysates were prepared from DND-39 cells stimulated with 10 ng ml $^{-1}$ of IL-4 for 24 h in the presence of 10 nM of TCDD for the indicated times. TCDD was added at the indicated times before cell harvest. Then western blotting was performed using either anti-AhR antibody or anti-Arnt antibody. (B) Cell lysates were prepared from DND-39 cells stimulated with 10 ng ml $^{-1}$ of IL-4 for 24 h. Ten nM of TCDD and 2 μM of MG132 were added 2 h before harvesting cells. Then western blotting was performed using either anti-AhR antibody or anti-Arnt antibody.

cells (Fig. 2B). Furthermore, induction of AhR by IL-4 was significantly decreased in spleen B cells derived from STAT6-deficient mice (Fig. 2C). These results demonstrated that AhR induction by IL-4 was mostly dependent on STAT6 activation.

Effects of TCDD and IL-4 on turnover of the AhR protein in B cells

It is known that the binding of a ligand to AhR triggers degradation of AhR by the ubiquitination/proteasome pathway in hepatocytes (23–25). To explore the possibility that this would also be the case with B cells, we analyzed the effect of TCDD and also IL-4 on turnover of the AhR protein in DND-39 cells. After AhR was induced by IL-4, incubation with TCDD for 6 h caused a significant decrease of AhR (Fig. 3A). We next tested the effects of MG132, a proteasomal inhibitor, on this TCDD-induced AhR degradation. We confirmed that co-incubation of 5 μM of MG132 with 10 nM of TCDD for 12 h completely recovered AhR degradation by TCDD in HepG2 cells, as previously reported (23) (data not shown). However, the same treatment by MG132 alone caused disappearance of both AhR and Arnt in DND-39 cells, indicating the non-specific inhibitory effect of MG132 at the transcription and/or translation level (data not shown). Therefore, we incubated IL-4-stimulated DND-39 cells with 2 μM of MG132 and 10 nM of TCDD for only 2 h. The treatment of 10 nM of TCDD for 2 h degraded AhR by almost half, and co-incubation of MG132 completely recovered AhR expression (Fig. 3B). In contrast, expression of the AhR protein, which was induced by IL-4, was sustained up to 48 h (data not shown). These results suggested that TCDD rapidly degraded the induced AhR protein through the proteasomal pathway in B cells, although IL-4 alone did not cause AhR degradation.

Nuclear location of AhR by IL-4 in B cells

It has been widely believed that AhR exists in the cytoplasm at the steady state and that binding to a ligand such as TCDD leads to translocation of AhR to the nuclei, followed by formation of the ternary complex for transcription together with Arnt (8, 9). We next explored the possibility that IL-4 alone would induce translocation of AhR from the cytoplasm to the nuclei. To address this question, we fractionated the cytoplasm and the nuclei of the cell lysates and then analyzed the amounts of AhR in each fraction. We used actin and HDAC1 as the marker proteins for the cytoplasmic and nuclear fractions, respectively. Based on the amounts of these proteins, no cytoplasmic protein was detected in the nuclear fraction, whereas the cytoplasmic fraction contained some nuclear protein in our system (Fig. 4). Upon stimulation of IL-4, AhR protein was observed in not only the cytoplasmic but also the nuclear fraction in DND-39 cells, demonstrating that IL-4 was able to induce AhR expression and translocate AhR to the nuclei. Co-culture with TCDD decreased the amount of AhR in the cytoplasmic fraction in both DND-39 cells and HepG2 cells by degradation through the ubiquitination/proteasome pathway; however, the amount of AhR in the nuclear fraction was sustained or increased in both DND-39 cells and HepG2 cells. These results indicated that IL-4 not only induced AhR but also translocated it to the nuclei and that although TCDD

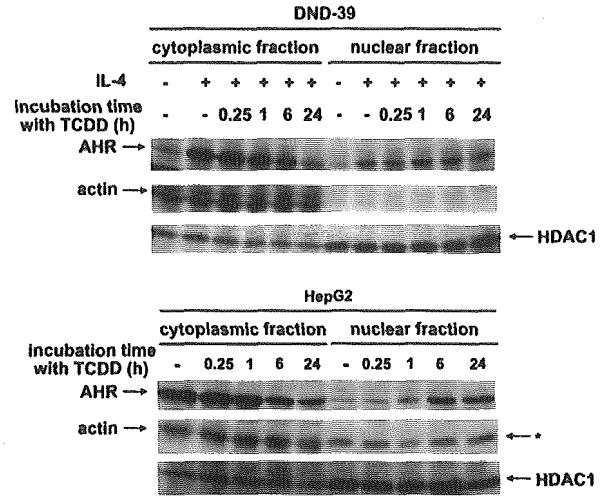

Fig. 4. Fractionation of AhR in the cytoplasm and nucleus. Cell lysates prepared from DND-39 cells and HepG2 cells stimulated with 10 ng ml $^{-1}$ of IL-4 for 24 h in the presence of 10 nM of TCDD for the indicated times were separated into cytoplasmic and nuclear fractions. Then western blotting was performed using either anti-AhR antibody or anti-actin antibody or anti-HDAC1 antibody. The asterisk depicts a non-specific band.

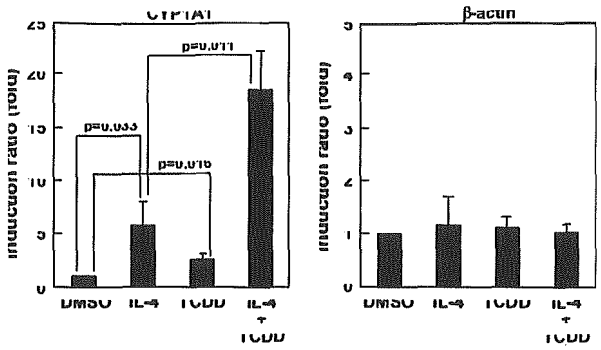

Fig. 5. Induction of CYP1A1 in DND-39 cells. Total RNA was extracted from DND-39 cells stimulated with 10 ng ml $^{-1}$ of IL-4 and/or 10 nM of TCDD for 24 h. Then real-time PCR analysis for CYP1A1 and β-actin was performed.

degraded AhR via the proteasomal pathway, the amounts of AhR in the nuclei were not affected in the presence of TCDD in DND-39 cells.

Induction of CYP1A1 by IL-4 and/or TCDD in B cells

It has been shown that several xenobiotic-metabolizing genes such as *CYP1A1*, *CYP1A2*, *CYP1B1* and *CYP2A8* are the main targets for the transcriptional complex of AhR and Arnt (8). Based on the present findings that IL-4 induced expression of AhR and translocated AhR into nuclei, we reasoned that AhR induced and activated by IL-4 in B cells would enhance induction of these CYP enzymes. When DND-39 cells were incubated with TCDD alone, the induction of CYP1A1 was very slight (~2-fold, Fig. 5). In the presence of both IL-4 and TCDD, expression of CYP1A1 was significantly enhanced (~18-fold). It is of note that IL-4 alone had the ability to cause CYP1A1 induction (~5-fold). As the cells were harvested after incubation with TCDD for 24 h, AhR protein was almost completely diminished by TCDD (Fig. 3A).

We next analyzed induction of CYP1A1 by IL-4 in mouse spleen B cells. When mouse spleen B cells were stimulated by TCDD alone, a slight induction of CYP1A1 occurred (~2-fold, Fig. 6A). In the presence of IL-4 and TCDD, significant induction of CYP1A1 as well as DND-39 cells was detected (~9-fold). Again, IL-4 alone induced several fold of CYP1A1 (~4-fold). Induction of CYP1A1 by IL-4 tended not to be observed, but rather decreased, in STAT6-deficient mice and AhR-deficient mice. Effects of TCDD remained in STAT6-deficient mice, but disappeared in AhR-deficient mice, as expected. CYP1B1 was induced in a way similar to CYP1A1 by IL-4 and/or TCDD, but the copy numbers of CYP1B1 were extremely low compared with those of CYP1A1 (data not shown). No induction of CYP1A2 was observed in mouse B cells (data not shown). β-Actin was slightly induced by IL-4 (~2-fold, Fig. 6B), and expression of ARNT was not affected by either IL-4 or TCDD (Fig. 6C). These results clearly demonstrated that AhR induced and translocated to nuclei by IL-4 in B cells was functional, inducing expression of a xenobiotic-metabolizing gene, *CYP1A1*, predominantly in B cells, and that TCDD exerted a synergistic effect on this induction.

Effect of AhR on IgE synthesis and CD23 expression

IgE synthesis and CD23 expression are major well-known functions of IL-4 on B cells. It has been already reported that TCDD, an environmental pollutant, enhances IgE synthesis in B cells (6, 7). To explore the possibility that AhR induced and activated by IL-4 was involved in expression of IgE and CD23, we compared the abilities to synthesize IgE and express CD23 in wild mice and AhR-deficient mice. Although when mouse B cells were stimulated with IL-4 and anti-CD40 antibody, significant IgE synthesis was observed, 5 pM of TCDD did not affect IgE synthesis and it was not impaired in AhR-deficient mice (Fig. 7A). CD23 expression was not affected by the presence of TCDD or in AhR-deficient mice (Fig. 7B). Furthermore, neither was human IgE synthesis induced by IL-4, anti-IgM antibody and anti-CD40 antibody affected by the co-culture with up to 1 nM of TCDD, nor was CD23 expression by IL-4 influenced by TCDD (data not shown). These results indicated that expression of AhR had no effect on IgE synthesis or CD23 expression induced by IL-4 in B cells.

Discussion

We report here our use of microarray analysis to identify IL-4- or IL-13-inducible genes in B cells, finding that the *AHR* gene was included in the list (data not shown). Because it is known that IL-4 and IL-13 play central roles in the pathogenesis of bronchial asthma (1, 4, 26), microarray technology has been applied to identify the downstream of IL-4 or IL-13 in several cells including bronchial epithelial cells, smooth muscle cells, lung fibroblasts and macrophages (13, 27–29) or in lung tissues derived from asthmatic monkeys induced by IL-4 (30).

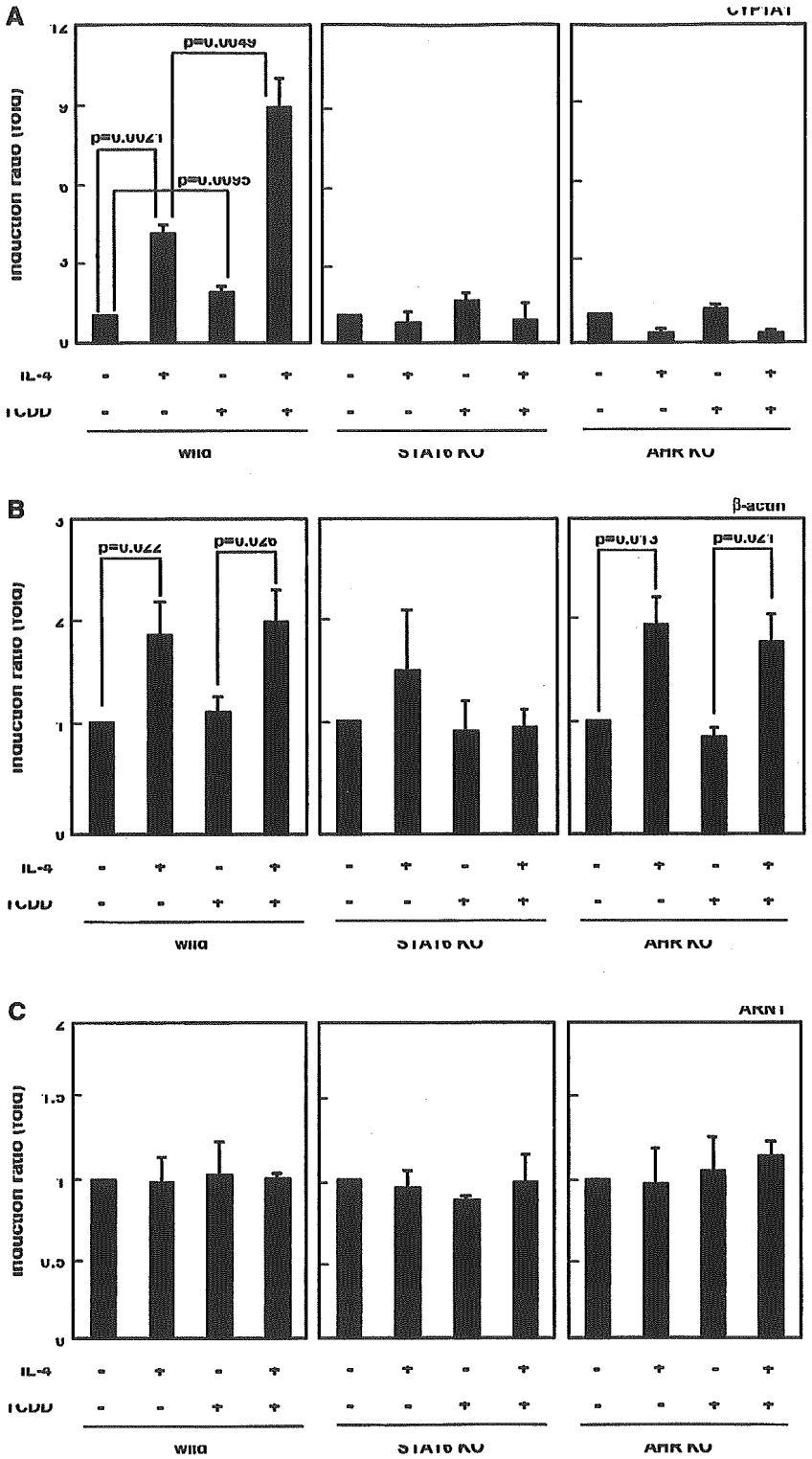

Fig. 6. Induction of CYP1A1 in mouse B cells. Total RNA was extracted from spleen B cells derived from wild mice, STAT6-deficient mice or AhR-deficient mice of C57/BL6 strain stimulated with 10 ng ml ^{1} of IL-4 and/or 5 pM of TCDD for 24 h. Then real-time PCR analysis for CYP1A1 (A), β-actin (B) and Arnt (C) was performed.

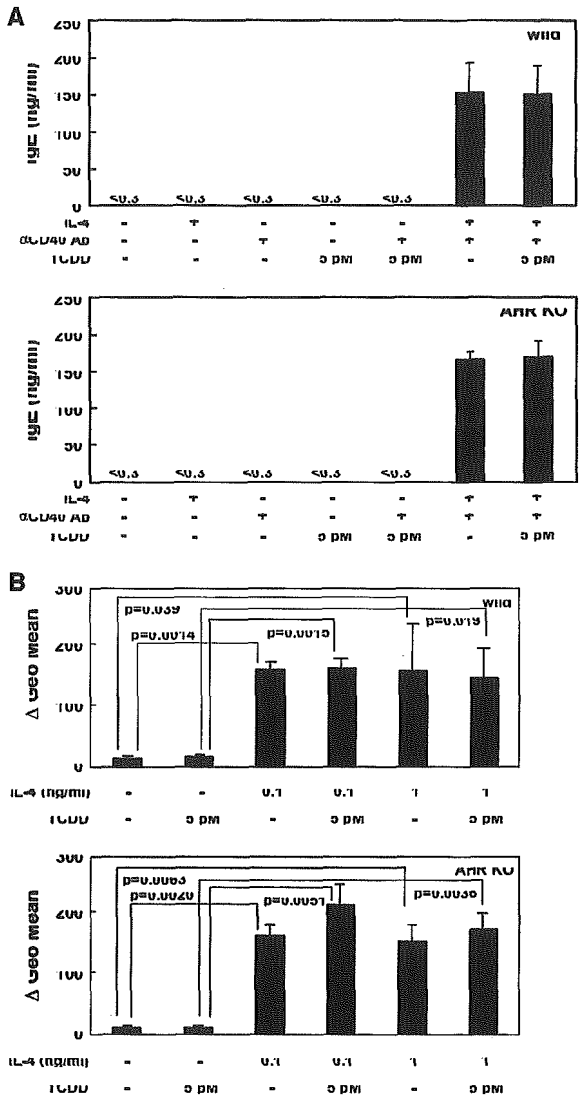

Fig. 7. Effect of AhR on IgE synthesis and CD23 expression in B cells. Spleen cells derived from wild mice or AhR-deficient mice of C57/BL6 strain were cultured with 1 ng ml $^{-1}$ of IL-4 and 0.5 μg ml $^{-1}$ of anti-CD40 antibody (only A) in the presence of 5 pM of TCDD for 5 days (A) or 24 h (B). Then the amounts of IgE in the supernatant (A) or the expression of CD23 on the surface (B) was assayed.

However, thus far, there is no application of microarray to identify IL-4- or IL-13-inducible genes in B cells. Our present microarray analysis has provided us a novel biological function of IL-4/IL-13 on B cells.

It has been already known that AhR is expressed in human tonsils (31); however, in this article, we demonstrated that AhR was induced and activated by IL-4 in B cells (Figs 1 and 4). In contrast, it has been reported that TCDD, a ligand for AhR, augments IgE synthesis in B cells (6, 7). Considering these results, it was assumed that IL-4/IL-13 and TCDD synergistically act on IgE synthesis in B cells, exaggerating allergic reactions. However, our present results denied this possibility because TCDD had no effect on IgE synthesis and CD23 expression by IL-4 in B cells (Fig. 7). In contrast, IL-4 could induce a xenobiotic-metabolizing gene, *CYP1A1*, among a number of gene products known to be regulated by AhR (Figs 5 and 6). These data suggested that IL-4 and IL-13 would have a role in metabolizing xenobiotics, including polycyclic aromatic hydrocarbons in B cells, which is a novel biological function of these cytokines.

In this article, we demonstrated that IL-4 had an ability not only to induce AhR, but also to activate AhR (Figs 1 and 4–6). Induction of AhR was dependent on STAT6, which is known to be critical for most of the biological activities of IL-4 or IL-13 (21, 22, 32) (Fig. 2). It would be possible that STAT6 binds to the promoter region of the *AHR* gene, enhancing its induction because the 5′-flanking region of the *AHR* gene has a consensus STAT6-binding motif (TTCCTGTGAA: 1721 to 1730 nucleotides from the translation start site). The present finding that AhR induction did not require *de novo* protein synthesis (Fig. 1B) would suggest that STAT6 might bind to this site and be involved in the induction of AhR.

It has already been shown that TCDD degrades AhR via the proteasomal pathway, and ubiquitination of AhR triggers this event (23–25, 33). We demonstrated that TCDD rapidly degraded IL-4-induced AhR through the proteasomal pathway in DND-39 cells as well as HepG2 cells (Fig. 3). In contrast, IL-4 alone could cause translocation of AhR into the nuclei, sustaining expression of AhR and inducing expression of CYP1A1 (Figs 4–6). These findings suggested that the nuclear translocation of AhR and the formation of the ternary transcriptional complex are not enough to trigger degradation of AhR but that binding of a ligand, such as TCDD, to AhR would be needed for this event. It is assumed that binding of a ligand to AhR may change its conformation, exposing the recognition site for the ubiquitination machinery. Thus, the activation mechanism of AhR is thought to be different between its ligands and IL-4 in that its ligands, but not IL-4 causes degradation of AhR, although both induce translocation of AhR into the nuclei.

In conclusion, we found that IL-4 could induce and activate AhR, inducing a xenobiotic-metabolizing gene, *CYP1A1*, in B cells. However, the induction of AhR had no effect on IgE synthesis or CD23 expression. These results indicate that the metabolism of xenobiotics by inducing and activating AhR would be a novel biological function of IL-4 and IL-13 in B cells, whereas TCDD is not involved in IgE synthesis in B cells.

Acknowledgements

We thank Dovie R. Wylie for a critical review of the manuscript. This work was supported in part by a Research Grant for Immunology, Allergy and Organ Transplant from the Ministry of Health, Welfare, and Labor of Japan, a grant-in-aid for Scientific Research from Japan Society for the Promotion of Science and AstraZeneca Research Grant 2002.

Abbreviations

AhR	aryl hydrocarbon receptor
Arnt	aryl hydrocarbon receptor nuclear translocator

CYP1A1	cytochrome P4501A1
HA-STAT6DN	hemagglutinin-tagged truncated form of STAT6
HDAC1	histone deacetylase class 1
RT	reverse transcription
TCDD	2,3,7,8-tetra-chlorodibenzo-*p*-dioxin

References

1 Izuhara, K., Arima, K. and Yasunaga, S. 2002. IL-4 and IL-13: their pathological roles in allergic diseases and their potential in developing new therapies. *Curr. Drug Targets Inflamm. Allergy* 1:263.

2 Zurawski, G. and de Vries, J. E. 1994. Interleukin 13, an interleukin 4-like cytokine that acts on monocytes and B cells, but not on T cells. *Immunol. Today* 15:19.

3 Chomarat, P. and Banchereau, J. 1998. Interleukin-4 and interleukin-13: their similarities and discrepancies. *Int. Rev. Immunol.* 17:1.

4 de Vries, J. E. 1998. The role of IL-13 and its receptor in allergy and inflammatory responses. *J. Allergy Clin. Immunol.* 102:165.

5 Kay, N. E. and Pittner, B. T. 2003. IL-4 biology: impact on normal and leukemic CLL B cells. *Leuk. Lymphoma* 44:897.

6 Takenaka, H., Zhang, K., Diaz-Sanchez, D., Tsien, A. and Saxon, A. 1995. Enhanced human IgE production results from exposure to the aromatic hydrocarbons from diesel exhaust: direct effects on B-cell IgE production. *J. Allergy Clin. Immunol.* 95:103.

7 Kimata, H. 2003. 2,3,7,8-Tetrachlorodibenzo-*p*-dioxin selectively enhances spontaneous IgE production in B cells from atopic patients. *Int. J. Hyg. Environ. Health* 206:601.

8 Sogawa, K. and Fujii-Kuriyama, Y. 1997. Ah receptor, a novel ligand-activated transcription factor. *J. Biochem. (Tokyo)* 122:1075.

9 Schmidt, J. V. and Bradfield, C. A. 1996. Ah receptor signaling pathways. *Annu. Rev. Cell Dev. Biol.* 12:55.

10 Puga, A., Xia, Y. and Elferink, C. 2002. Role of the aryl hydrocarbon receptor in cell cycle regulation. *Chem. Biol. Interact.* 141:117.

11 Tian, Y., Rabson, A. B. and Gallo, M. A. 2002. Ah receptor and NF-κB interactions: mechanisms and physiological implications. *Chem. Biol. Interact.* 141:97.

12 Umeshita-Suyama, R., Sugimoto, R., Akaiwa, M. *et al.* 2000. Characterization of IL-4 and IL-13 signals dependent on the human IL-13 receptor α chain 1: redundancy of requirement of tyrosine residue for STAT3 activation. *Int. Immunol.* 12:1499.

13 Yuyama, N., Davies, D. E., Akaiwa, M. *et al.* 2002. Analysis of novel disease-related genes in bronchial asthma. *Cytokine* 19:287.

14 Izuhara, K., Heike, T., Otsuka, T. *et al.* 1996. Signal transduction pathway of interleukin-4 and interleukin-13 in human B cells derived from X-linked severe combined immunodeficiency patients. *J. Biol. Chem.* 271:619.

15 Yagi, R., Nagai, H., Iigo, Y., Akimoto, T., Arai, T. and Kubo, M. 2002. Development of atopic dermatitis-like skin lesions in STAT6-deficient NC/Nga mice. *J. Immunol.* 168:2020.

16 Mimura, J., Yamashita, K., Nakamura, K. *et al.* 1997. Loss of teratogenic response to 2,3,7,8-tetrachlorodibenzo-*p*-dioxin (TCDD) in mice lacking the Ah (dioxin) receptor. *Genes Cells* 2:645.

17 Yasunaga, S., Yuyama, N., Arima, K. *et al.* 2003. The negative-feedback regulation of the IL-13 signal by the IL-13 receptor α2 chain in bronchial epithelial cells. *Cytokine* 24:293.

18 Gaff, C., Grumont, R. J. and Gerondakis, S. 1992. Transcriptional regulation of the germline immunoglobulin C α and C ε genes: implications for commitment to an isotype switch. *Int. Immunol.* 4:1145.

19 Yokota, A., Kikutani, H., Tanaka, T. *et al.* 1988. Two species of human Fc ε receptor II (Fc ε RII/CD23): tissue-specific and IL-4-specific regulation of gene expression. *Cell* 55:611.

20 Marcus, R. S., Holsapple, M. P. and Kaminski, N. E. 1998. Lipopolysaccharide activation of murine splenocytes and splenic B cells increased the expression of aryl hydrocarbon receptor and aryl hydrocarbon receptor nuclear translocator. *J. Pharmacol. Exp. Ther.* 287:1113.

21 Takeda, K., Tanaka, T., Shi, W. *et al.* 1996. Essential role of Stat6 in IL-4 signaling. *Nature* 380:627.

22 Shimoda, K., van Deursen, J., Sangster, M. Y. *et al.* 1996. Lack of IL-4-induced Th2 response and IgE class switching in mice with disrupted Stat6 gene. *Nature* 380:630.

23 Davarinos, N. A. and Pollenz, R. S. 1999. Aryl hydrocarbon receptor imported into the nucleus following ligand binding is rapidly degraded via the cytosplasmic proteasome following nuclear export. *J. Biol. Chem.* 274:28708.

24 Roberts, B. J. and Whitelaw, M. L. 1999. Degradation of the basic helix-loop-helix/Per-ARNT-Sim homology domain dioxin receptor via the ubiquitin/proteasome pathway. *J. Biol. Chem.* 274:36351.

25 Ma, Q. and Baldwin, K. T. 2000. 2,3,7,8-Tetrachlorodibenzo-*p*-dioxin-induced degradation of aryl hydrocarbon receptor (AhR) by the ubiquitin-proteasome pathway. Role of the transcription activaton and DNA binding of AhR. *J. Biol. Chem.* 275:8432.

26 Wills-Karp, M. and Chiaramonte, M. 2003. Interleukin-13 in asthma. *Curr. Opin. Pulm. Med.* 9:21.

27 Lee, J. H., Kaminski, N., Dolganov, G. *et al.* 2001. Interleukin-13 induces dramatically different transcriptional programs in three human airway cell types. *Am. J. Respir. Cell Mol. Biol.* 25:474.

28 Syed, F., Panettieri, R. A., Jr, Tliba, O. *et al.* 2005. The effect of IL-13 and IL-13R130Q, a naturally occurring IL-13 polymorphism, on the gene expression of human airway smooth muscle cells. *Respir. Res.* 6:9.

29 Welch, J. S., Escoubet-Lozach, L., Sykes, D. B., Liddiard, K., Greaves, D. R. and Glass, C. K. 2002. TH2 cytokines and allergic challenge induce Ym1 expression in macrophages by a STAT6-dependent mechanism. *J. Biol. Chem.* 277:42821.

30 Zou, J., Young, S., Zhu, F. *et al.* 2002. Microarray profile of differentially expressed genes in a monkey model of allergic asthma. *Genome Biol.* 3:research0020.1.

31 Lorenzen, A. and Okey, A. B. 1991. Detection and characterization of Ah receptor in tissue and cells from human tonsils. *Toxicol. Appl. Pharmacol.* 107:203.

32 Takeda, K., Kamanaka, M., Tanaka, T., Kishimoto, T. and Akira, S. 1996. Impaired IL-13-mediated functions of macrophages in STAT6-deficient mice. *J. Immunol.* 157:3220.

33 Santiago-Josefat, B., Pozo-Guisado, E., Mulero-Navarro, S. and Fernandez-Salguero, P. M. 2001. Proteasome inhibition induces nuclear translocation and transcriptional activation of the dioxin receptor in mouse embryo primary fibroblasts in the absence of xenobiotics. *Mol. Cell. Biol.* 21:1700.

Arch Toxicol (2005) 79: 260–267
DOI 10.1007/s00204-004-0626-4

MOLECULAR TOXICOLOGY

Noriko Nishimura · Junzo Yonemoto · Yuichi Miyabara
Yoshiaki Fujii-Kuriyama · Chiharu Tohyama

Altered thyroxin and retinoid metabolic response to 2,3,7,8-tetrachlorodibenzo-*p*-dioxin in aryl hydrocarbon receptor-null mice

Received: 24 July 2004 / Accepted: 5 October 2004 / Published online: 17 November 2004

Abstract To determine whether the disruption of thyroid hormone and retinoid homeostasis that occurs after exposure to 2,3,7,8-tetrachlorodibenzo-*p*-dioxin (TCDD) can be mediated by the arylhydrocarbon receptor (AhR), pregnant AhR-heterozygous (AhR+/) mice were administered a single oral dose of 10 μg kg ^{1} TCDD at gestation day 12.5. Serum and liver were collected on postnatal day 21 from vehicle-treated control or TCDD-treated AhR+/ and AhR-null (AhR /) mouse pups. Whereas TCDD exposure resulted in a marked reduction of total thyroxin (TT4) and free T4 (FT4) levels in the serum of AhR+/ mice, TCDD had no e ects on AhR / mice. Gene expression of UDP-glucuronosyltransferase (UGT)1A6, cytochrome P450 (CYP)1A1, and CYP1A2 in the liver was induced markedly by TCDD in AhR+/ but not AhR / mice. Induction of CYP1A1 in response to TCDD was confirmed by immunohistochemical evidence in that CYP1A1 protein was conspicuously localized in the cytoplasm of hepatocytes in the centrilobular region. Levels of retinyl palmitate were greatly reduced in the liver of TCDD-exposed AhR+/ mice, but not in vehicle-treated AhR+/ mice. No e ects of TCDD on retinoid levels in the liver were found in AhR / mice. We conclude that disruption of thyroid hormone and retinoid homeostasis is mediated entirely via AhR. Induction of UGT1A6 is thought to be responsible at least partly for reduced serum thyroid hormone levels in TCDD-exposed mice.

Keywords Aryl hydrocarbon receptor-null mice · Retinoid · Thyroxin · 2,3,7,8-Tetrachlorodibenzo-*p*-dioxin · Vitamin A

N. Nishimura (✉) · J. Yonemoto
Endocrine Disruptors and Dioxin Research Project,
National Institute for Environmental Studies,
305-8506 Tsukuba, Japan
E-mail: nishimura.noriko@nies.go.jp
Fax: +81-298-50-2561

Y. Miyabara
Research and Education Center for Inlandwater Environment,
Shinshu University, Suwa, 392-0027 Nagano, Japan

Y. Fujii-Kuriyama
Center for Tsukuba Advanced Research Alliance,
University of Tsukuba, 305-8577 Tsukuba, Japan

C. Tohyama
Environmental Health Sciences Division,
National Institute for Environmental Studies,
305-8506 Tsukuba, Japan

Introduction

Dioxin and dioxin-like polychlorinated biphenyls (PCBs) are ubiquitously present in the environment, and 2,3,7,8-tetrachlorodibenzo-*p*-dioxin (TCDD) is the most potent congener among a large family of dioxin compounds. Exposure to TCDD results in reproductive, immunological, and neurobehavioral toxicities, teratogenicity and carcinogenicity. Among these toxicities, e ects on thyroid hormone metabolism is a major concern in humans because of epidemiological studies which suggest a possible link between these e ects and environmental exposure to dioxin and related compounds (Koopman-Esseboom et al. 1994, 1996).

Thyroid hormone is required for brain development and neuronal maintenance and has metabolic functions during the fetal and early neonatal periods. Exposure to TCDD has been shown to cause morphological and functional disorders of the thyroid of laboratory animals. The most consistent e ect of TCDD exposure in mammals is a marked decrease in serum T4 concentrations (Brucker-Davis 1998). Administration of a single exposure to TCDD increased remarkably the intensity of immunostaining of T4 and TSH accompanied by hyperplasia of thyroid follicular cells in Sprague–Dawley rats, suggesting that the continuous excessive secretion of TSH caused by the perturbation of the thyroid-pituitary axis by TCDD leads to proliferative changes in

thyroid follicular cells (Nishimura et al. 2002). The thyroid hyperplasia due to disruption of thyroid hormone homeostasis was shown in the thyroid of pups born to Holtzman rat dams exposed to TCDD on gestational day (GD) 15 (Nishimura et al. 2003). However, whether the mechanism(s) responsible for functional alterations in thyroid can be mediated by the arylhydrocarbon receptor (AhR) has not been examined.

It has been established that binding to the AhR is the first necessary step for TCDD to exert its toxic e ects. TCDD subsequently translocates into the nucleus, and then forms a heterodimer with the arylhydrocarbon receptor nuclear translocator. This ligand-receptor translocator complex is bound to the xenobiotic responsive element of the promoter region of target genes and accelerates transcription activity (Gonzalez and Fernandez-Salguero 1998). After production of three di erent colonies of AhR-null mice by homologous recombination, it is proven that AhR is responsible for most of the toxicities caused by TCDD so far examined, such as thymic involution and hepatic development (Fernandez-Salguero et al. 1996), cleft palate, and hydronephrosis (Mimura et al. 1997; Peters et al. 1999).

A very close relationship between disturbances of vitamin A homeostasis and toxicity of dioxin was first suggested because of the similar symptoms of dioxin-exposed and vitamin A-deficient animals (Innami et al. 1974). Exposure to TCDD was shown to decrease retinol and retinyl ester concentrations and the amounts of esterified storage form of vitamin A in the liver, with a significant enhancement of urinary excretion of retinoid derivatives (Brouwer et al. 1989) and in serum and kidney retinoic acid levels (Nilsson et al. 2000).

AhR seems to be involved in vitamin A homeostasis. An inverse relationship between CYP1A1 induction and hepatic vitamin A concentration suggested an AhR-mediated biochemical process in the altered vitamin A homeostasis after TCDD-dosing (Fletcher et al. 2001). Compared to AhR wild-type mice, AhR-null mice showed a three-fold increase in hepatic levels of retinyl palmitate and a three-fold accumulation in retinoic acid and retinol (Andreola et al. 1997). Di erences between how various PCB congeners altered vitamin A homeostasis depended on the a nity for the AhR (Chen et al. 1992).

The activity field and signaling pathway of retinoids and thyroid hormones are closely related (Schrader and Carlberg 1994; Chin and Yen 1997), and both retinoids and thyroid hormones play critical roles in the normal development of the central nervous system (Maden et al. 1998). In women su ering from hyper- or hypothyroidism, functional disorder of the thyroid has been shown to change retinoid levels in serum (Umesh and Shobhita 1999).

Changes in vitamin A and thyroid hormone levels are well-known e ect of dioxins in rodents, which have been suggested as sensitive biomarkers of exposure to dioxins. Increased oxidation and glucuronidation of retinoids by enzymes such as CYP1A1 and UDPG (both regulated by AhR) contributes to decreased hepatic vitamin A levels following exposure to dioxins. Thyroid hormones and retinol are transported in the blood on the same carrier protein complex, transthyretin (TTR), a 55-kDa tetrametric protein having high a nity binding sites for T3 and T4 in rodents. A macromolecular complex formed by binding with retinol-binding protein (RBP) prevents renal glomerular filtration of the RBP–retinol complex. Competitive binding of hydroxylated metabolites of PCB to TTR might be responsible for a decrease in plasma levels of thyroid hormones, RBP, and retinol.

This study was designed to explore the role of the AhR in thyroid dysfunction and in the disturbance of vitamin A metabolism in response to TCDD, using AhR-null mice.

Materials and methods

Animals and TCDD treatment

AhR / mice were generated by using a homologous recombination method as described previously (Mimura et al. 1997). Male AhR+/ were backcrossed to C57BL/6 J AhR+/+ female mice. The genotype of each pup was determined by analyzing the presence of the mutant AhR allele by PCR with genomic DNA taken from the tail. Pups were housed in a room at 23 ± 1 C, 50 ± 10% humidity, on a 12-h light–dark cycle. The animals received laboratory rodent chow and distilled water ad libitum, and were handled with humane care under the guidelines on animal experiments of the National Institute for Environment Studies (NIES). Ten-week-old AhR+/ female mice in proestrus were mated 1:1 with AhR+/ males overnight, and the days when female mice had vaginal plugs the following morning were designated as day 0 of gestation. Pregnant mice (AhR+/) were administered a single oral dose of 10 μg kg ^{1} TCDD at gestation day 12.5. Control mice (AhR+/) received an equivalent volume of corn oil. Because we did not obtain enough AhR wild-type mice (AhR+/+), only AhR heterozygous (AhR+/) and AhR-null (AhR /) mice were used in this experiment.

Serum and liver from AhR+/ or AhR / pups were collected on postnatal day 21 and analyzed. Tissues were fixed in Zamboni's solution for 24 h at 4 C and processed for immunohistological examination. For biochemical examination, tissues were snap-frozen in liquid nitrogen and stored at 80 C until further processing.

Thyroid hormone analysis

Serum total T4 (TT4) and free T4 (FT4) levels were quantified with Amerlex radioimmunoassay kits (Amersham, Buckinghamshire, UK) according to the manufacturer's instructions.

RNA extraction and RT-PCR

Total hepatic RNA was extracted by using Isogen (Nippon Gene, Tokyo, Japan). The integrity of the RNA was assessed by agarose gel electrophoresis followed by ethidium bromide staining, and the quantity was determined by absorbance at 260 and 280 nm. Expression of CYP1A1, CYP1A2, UGT1A6, and β-actin was determined by reverse transcription–polymerase chain reaction (RT-PCR) using PCR primers (Table 1) for amplification according to a procedure described previously (Nishimura et al. 2002) with some modification. RT for RNA was performed in a final volume of 20 μL containing 5.0 mmol L^{-1} $MgCl_2$, 1.0 mmol L^{-1} dNTP, 0.25 U μL^{-1} AMV reverse transcriptase, 0.125 μmol L^{-1} oligo dT-adaptor primer, 1 U μL^{-1} RNase inhibitor, and 1 μg total RNA, using RNA LA PCR kit (Takara, Otsu, Japan). The RT samples were incubated at 42 C for 15 min and then at 99 C for 5 min for inactivation of RTase. PCR was subsequently performed as follows: the reaction was run at 94 C for 2 min, amplified by using temperatures of 94 C for 30 s, 56 C for 30 s, and 72 C for 30 s, with 24 cycles applied for UGT1A6, CYP1A2 and β-actin and 20 cycles for CYP1A1. The PCR mixture (10 μL) contained 2.5 mmol L^{-1} $MgCl_2$, 0.25 U Takara LA Taq, 0.2 μM of each forward and reverse primer, and 2 μL RT products. PCR products were detected as a single band on 1.5% agarose gel in 1×TBE containing 2 μg mL^{-1} ethidium bromide. Band intensity was quantified by EDAS 290 system Version 3.5.3 (Kodak, Rochester, NY, USA).

Immunohistochemistry

Tissue sections of liver were stained for CYP1A1 by an indirect immunohistochemical technique described previously (Nishimura et al. 2000). Briefly, after depara - nization and rehydration, tissue sections were heated twice for 1 min at the maximum power setting (980 W) of a microwave oven with 40–45 s boiling time (0.01 mol L^{-1} sodium citrate bu er; pH 6.0). After microwave pretreatment, the sections were washed in PBS for 5 min and endogenous peroxidase activity was quenched by incubation in 0.3% H_2O_2 in methanol. Goat polyclonal antibody (CYP1A1, G 18: sc-9828) raised against a peptide mapping near the carboxyl terminus of CYP1A1 of mouse origin (Santa Cruz Biotechnology, Santa Cruz, CA, USA) was diluted 1:200 in PBS. After incubating 2% normal goat serum with the sections, the primary antibody was incubated over the section in a humidified chamber for 1 h at 37 C. After washing sections with PBS, they were incubated for 1 h with biotinylated rabbit anti-goat IgG (BA-1000; Vector Laboratory, Burlingame, CA, USA) diluted 1:300 in PBS. The sections were then washed and incubated for 30 min with an avidin-biotinylated peroxidase complex (PK-4000, Vector Laboratory). Immunoreactions were performed using hydrogen peroxide-activated 3,3′-diaminobenzodine tetrahydrochloride (Sigma, St Louis, MO, USA). Negative controls, in which the primary antibody was replaced with normal goat IgG, did not show nonspecific staining.

Analysis of retinoids by HPLC

Hepatic retinoid analysis was performed as described by Got et al (1995) with some modification. Retinoids from liver homogenates were extracted with *n*-hexane and analyzed by HPLC (Model 2690; Waters, West Lothian, UK), monitoring fluorescence at 340 nm (excitation) and 460 nm (emission) by fluorescence detector (Model 474; Waters). Retinol, retinyl palmitate, and other retinyl esters were quantified on the basis of calibration curves using retinol or retinyl palmitate as standards.

Statistical analysis

StatView for Windows (version 5.0; SAS Institute, Cary, NC, USA) was used for statistical analysis. Values are expressed as means ± SEM for individual groups of animals. Di erences between means among experimental groups was assessed by analysis of variance; mean values for AhR+/ and AhR / mice were compared by Student's *t*-test. *P* values less than 0.05 were considered statistically significant.

Results

E ects of TCDD on serum thyroid hormone concentrations and expression of TCDD-target genes in AhR+/ mice and AhR / mice

TCDD exposure drastically decreased serum TT4 and FT4 concentrations in AhR+/ mice compared with

Table 1 PCR primer name, sequence, and product size

Primer		Sequence (5′ to 3′)	Size (bp)
CYP1A1	ForwardReverse	CCATGACCGGGAACTGTGGTCTGGTGAGCATCCTGGACA	344
UGT1A6	ForwardReverse	CTTCCTGCAGGGTTTCTCTTCCCAACGATGCCATGCTCCCC	875
CYP1A2	ForwardReverse	CAGTATCCAAGACATCACAAGTGTGTATCGGTAGATCTCCAG	301
β-actin	ForwardReverse	CCTCTATGCCAACACAGTAGCCACCGATCCACACAG	153

vehicle-treated control mice, but no alterations were found in TCDD-exposed AhR / mice (Figs. 1a, b). No sexual di erences in serum TT4 and FT4 levels were found as a result of di erent TCDD exposure.

Using semi-quantitative RT-PCR, we found that gene expression of hepatic CYP1A1 was markedly induced in TCDD-exposed AhR +/ mice, but not in TCDD-exposed AhR / mice. TCDD exposure also induced UGT1A6 and CYP1A2 expression in livers of AhR +/ mice compared with vehicle-treated AhR +/ mice, while no e ects of TCDD were observed in AhR / mice (Figs. 2b, c, d). Male and female animals responded to TCDD similarly for these three genes.

We next examined changes in immunohistochemical localization of CYP1A1 in the liver of TCDD-exposed AhR +/ mice and AhR / mice. No immunostaining of hepatic CYP1A1 was observed in vehicle-treated AhR +/ mice (Fig. 3c) and TCDD-treated AhR / mice (Fig. 3d), but an increase in the intensity of cytoplasmic staining of CYP1A1 was observed clearly in TCDD-treated AhR +/ mice (Figs. 3a, b). Staining for CYP1A1 was localized mainly in hepatocytes surrounding the central vein.

E ects of TCDD on hepatic vitamin A in AhR +/ mice and AhR / mice

We determined the concentrations of vitamin A derivatives that accumulated in the liver of vehicle-treated AhR +/ mice, and retinoids in the liver were confirmed to consist of retinyl palmitate (approx. 90%) and retinol (Fig. 4a). TCDD treatment resulted in approximately 50% and 21% decrease in retinyl palmitate and retinol levels, respectively, in AhR +/ mice in comparison with vehicle-treated AhR +/ mice (Figs. 4b and c). TCDD reduced a total retinoid level in AhR +/ mice to approximately 40% that of vehicle-treated AhR +/ mice (Fig. 4d). Although no statistically significant changes were found between AhR +/ mice and AhR / mice, there seemed a tendency for retinol palmitate, total retinoid, and retinol concentrations in AhR / mice to be higher than in AhR +/ mice.

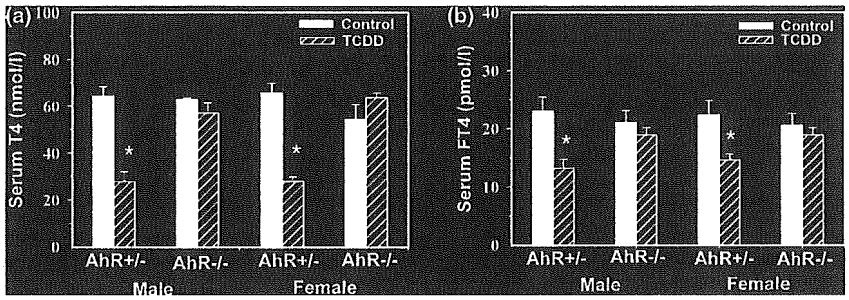

Fig. 1 E ects of TCDD on serum levels of total thyroxin (TT4) (**a**) and free thyroxin (FT4) (**b**) in AhR+/ and AhR / mice. TCDD exposure induced a significant reduction of serum levels of both TT4 and FT4 in AhR +/ but not AhR / mice. Values are means ± SEM ($n=6$). An *asterisk* indicates a significant di erence from vehicle controls ($P<0.05$)

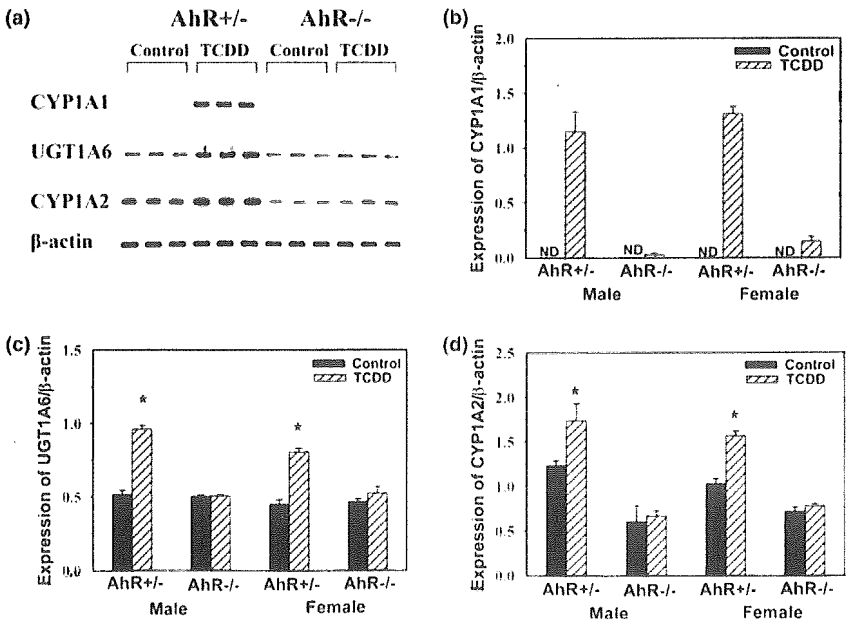

Fig. 2 RT-PCR analysis of CYP1A1 (**a** and **b**), UGT1A6 (**a** and **c**), and CYP1A2 (**a** and **d**) mRNA expression in the livers of AhR +/ or AhR / mice exposed to TCDD. Exposure to TCDD induced gene expression of CYP1A1 in AhR +/ but not in AhR / mice (both males and females). Hepatic UGT1A6 and CYP1A2A expression was induced significantly by TCDD exposure in AhR +/ but not AhR / mice. β-Actin was used to control the amount of mRNA loaded. Values are means ± SEM ($n=4$–6). An *asterisk* indicates significant di erence from vehicle controls ($P<0.05$)

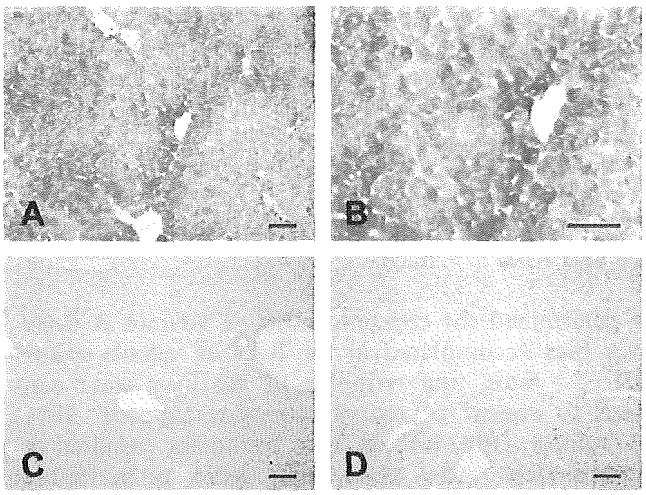

Fig. 3 Immunohistochemical location of CYP1A1 in the livers from AhR+/ or AhR / mice (postnatal day 21) exposed to TCDD. (**a**) Liver section from a representative TCDD-treated AhR+/ mouse, and (**b**) higher magnification of (**a**). Exposure to TCDD resulted in an increase in the number of hepatocytes strongly stained with antibody specific to CYP1A1. The stained hepatocytes were located around the centrilobular region. (**c**) Vehicle-treated AhR+/ mice showed almost no staining for CYP1A1 in the liver. (**d**) No staining for CYP1A1 was found in the liver from TCDD-treated AhR / mice. *Bar* = 50 μm

Discussion

It has been established that thyroid hormone plays a physiologically essential role in brain development, and disruption of thyroid hormone homeostasis has gained much attention for health risk assessment of dioxin and related compounds since epidemiological studies suggested association of cognitive ability and children's play preference with prenatal exposure to dioxin and related compounds (Vreugdenhil et al. 2002). It has been reported that thyroid hormone, T4, is conjugated with glucuronide by UGT1A1 and 1A6, a phase II drug-metabolizing enzyme, the genes of which have XRE motif(s) in the promoter region and are activated by liganded AhR-ARNT complex in the rat (Emi et al. 1996) and humans (Munzel et al. 1998). The extrathyroidal e ects of TCDD on thyroid hormone turnover were studied in the rodent, and induction of UGP-glucuronosyltransferase activity by TCDD was found to be primarily responsible for reducing circulating T4 levels by accelerated biliary excretion through enhanced T4-glucuronide formation (Ritter 2000).

In this study it was clearly demonstrated by two lines of evidence that disruption of thyroid hormone homeostasis by TCDD is mediated entirely via AhR. First, serum TT4 and FT4 concentrations were not changed in TCDD-exposed AhR / mice in contrast with a drastic reduction in AhR+/ mice. Such a reduction in laboratory animals has been shown in earlier studies (Brucker-Davis 1998; Nishimura et al. 2002). Second, expression of UGT1A6 was induced in AhR+/ mice but not in AhR / mice (Fig. 2c), which resulted in reduced T4 levels in blood circulation, because of increased biliary excretion of T4 glucuronide.

The induction and consequent localization of CYP1A1 in the liver after TCDD exposure is now clearly confirmed by comparing AhR+/ mice and AhR / null mice (Figs. 2 and 3). Immunostaining for CYP1A1 was visualized in the cytoplasm around the central vein. This hepatic distribution of the protein accords well with a previous study that showed induction of CYP1A1 mRNA and its protein predominantly in centrilobular hepatocytes rather than the periportal hepatocytes, in isolated hepatocytes (Santostefano et al. 1999), and in hepatic tissue sections (Tritscher et al. 1992). Santostefano et al. (1999) reported that centrilobular hepatocytes showed a 2.7- to 4.5-fold higher

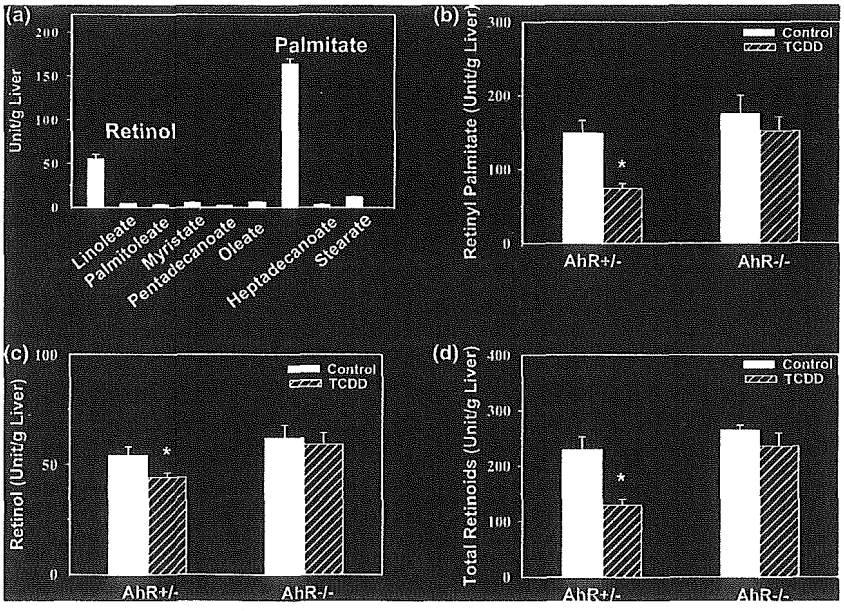

Fig. 4 E ects of TCDD on hepatic retinoid concentrations in AhR+/ mice and AhR / mice on postnatal day 21. (**a**) Hepatic retinoid content of vehicle-treated control mice. (**b**) Hepatic retinyl palmitate content of AhR+/ mice and AhR / mice. (**c**) Hepatic retinol content of AhR+/ and AhR / mice. (**d**) Hepatic total retinoid content of AhR+/ and AhR / mice. Values are means ± SEM ($n = 4$–5). An *asterisk* indicates a significant di erence from vehicle-treated controls ($P < 0.05$)

concentration of TCDD compared with periportal hepatocytes. This localization of CYP1A1 probably reflects di erences between TCDD distribution in liver.

Extensive studies have revealed that reduction of hepatic retinoid stores is one of the most sensitive indicators among TCDD-induced toxic manifestations. In this study we found that perturbation of vitamin A homeostasis by TCDD was clearly mediated by AhR. Pups born to TCDD-exposed AhR+/ dams had a marked reduction in retinyl palmitate, retinol, and total retinoid levels compared with vehicle-treated controls whereas the levels of neither of these three substances was a ected by TCDD exposure in AhR / mice (Fig. 4). Regarding basal levels of retinoids in the liver, Andreola et al. (1997) demonstrated a 2 to 3-fold higher retinoid concentrations in AhR / mice than AhR+/ + mice liver, and an intermediate value in AhR+/ mice. Although no such a clear-cut di erence was found in this study, at least partly because of di erent colonies of AhR / mice, levels of all three species, retinyl palmitate, retinol, and retinoids, in the liver of the AhR / pups born to vehicle-treated control dams seemed to be higher than those in AhR+/ mice (Fig. 4). A plausible explanation of this di erence between the two studies might be the use of di erent colonies of AhR / mice.

The mechanism(s) responsible for TCDD-induced reduction of hepatic retinoid levels remain unclear. Two plausible explanations have been proposed. The first hypothesis is that TCDD inhibits enzymes, for example lecithin:retinol acyltransferase and acyl Co-A:retinol acyltransferase, responsible for converting retinol to retinyl palmitate, and increases retinyl ester hydrolase that catalyzes degradation of retinyl ester, although it is not known whether the genes of these enzymes are regulated directly in an AhR-mediated manner. Nilsson et al. (2000) demonstrated an inhibitory e ect of TCDD on lecithin:retinol acyltransferase. Because, in this study, TCDD treatment was found to reduce not only retinyl palmitate, but also retinol levels in liver (Fig. 4), suppression of lecithin:retinol acyltransferase activity, if any, is unlikely to be a major contributing factor. Acyl Co-A:retinol acyltransferase is another enzyme involved in retinol esterification, but administration of TCDD did not a ect hepatic Acyl Co-A:retinol acyltransferase activity except at very high dose (100 μg TCDD kg ^{1}), suggesting this enzyme is not responsible for the decrease in retinol ester level in the liver (Nilsson et al. 2000). Because Nilsson et al. (2000) also did not find an increase in hepatic retinol ester hydrolase in rats treated with 10 μg kg ^{1}, the reduction of retinol ester in the liver in this study cannot be explained by the hydrolysis pathway. These findings on TCDD exposure suggest that enzymes that catalyze either synthesis or degradation of retinyl ester do not necessarily result in the reduction of hepatic retinoid stores.

An alternative hypothesis has been sought to explain the disturbance of retinoid homeostasis by TCDD. Although several hypotheses have been proposed to explain the impaired vitamin A kinetics by TCDD, a generally accepted view is that a decrease in retinoid stores in liver results from increased catabolism, mobilization, and elimination of hepatic retinoids (Brouwer et al. 1989; Kelly et al. 1998; Nilsson and Hakansson 2002). Retinol and retinoic acid can be metabolized via cytochrome P450 enzyme systems to inactive metabolites; subsequently, glucuronized compounds would contribute to increases in urinary and fecal excretion of polar vitamin A metabolites following TCDD exposure. The deficiency of the ability of AhR-null mice to catabolize retinoic acid via P450 enzymes contributes to an increased level of retinoic acid in the liver of AhR-null mice (Gonzalez and Fernandez-Salguero 1998). It is thus thought that lack of CYP1A1 enzyme due to inactivation of AhR might prevent vitamin A excretion. However, there is a large body of evidence that retinoids are subject to glucuronidation, leading to increased elimination into the bile (Zile et al. 1980, 1982). A decrease in hepatic stores of retinyl palmitate after TCDD exposure might result from an increased level of glucuronidation. Bank et al. (1989) found reduced retinoid levels in liver and an increase in hepatic UGT activity after TCDD exposure and verified in-vitro formation of retinyl beta-glucuronide.

Recently, Schmidt et al. (2003) observed dose-dependent elevation of all-trans-retinoic acid levels in the liver of male Sprague–Dawley rats exposed to TCDD at doses ranging from 0.1 to 100 μg kg ^{1} body weight. In this study, 9-*cis*-4-oxo-13,14-dihydro-RA was drastically decreased by TCDD in a dose-dependent manner, but protein and mRNA levels of cellular retinol binding protein I (CRBP-I) in liver were not significantly altered by TCDD exposure at doses at which retinoid levels were a ected, making CRBP-I an unlikely candidate to account for alterations in retinoid metabolism caused by TCDD. The authors concluded that among relevant cytochrome P450 (CYP) enzymes with potential roles in all-*trans*-RA synthesis and/or degradation (CYP1A1, 1A2, and 2B1/2), CYP1A1 is suggested as responsible for TCDD-induced all-*trans*-RA synthesis in liver and other tissues (Schmidt et al. 2003).

UGTs are enzymes that catalyze the conjugation of xenobiotics and endogenous compounds with UDP-glucuronic acid and play a crucial role in the deactivation and excretion of those compounds.

The UGT1A family is selectively induced by both MC and TCDD. The AhR is necessary for expression of MC and TCDD toxic manifestations and participates in glucuronidation of retinoids (Bank et al. 1989). Retinoid glucuronidation induced by MC was catalyzed by an MC-inducible UGT isozyme (Sass et al. 1994). Although seven isozymes are known to belong to the UGT1 family in rat (Ritter 2000), only UGT1A6 and UGT1A7 were induced by MC and PCB, which strongly supports the notion that UDP-glucuronosyltransferases are responsible for the biotransformation of retinoid in the tissue. Recent studies using AhR-null mice suggested the presence of a novel pathway of negative feedback regulation of RA synthesis from retinal via aldehyde dehydroge-

nase 1 (Elizondo et al. 2000). More recently, Andreola et al. (2004) reported that CYP2C39, which acts as a retinoic acid 4-hydroxylase in the liver, is down-regulated in the AhR / mice compared with AhR+/+ mice, and thus responsible for disturbance of retinoid homeostasis in the AhR-null mice. However, the expression of genes that encode these enzymes were not a ected by TCDD exposure in AhR+/+ mice. Thus, the present observation of a marked decrease in retinoid levels in the liver would have been caused by yet unidentified mechanism. Thus, it is still necessary to identify and characterize the genes and their products that are responsible for direct and indirect XRE-driven retinoid metabolism.

Acknowledgements We thank Drs S. Osako, H. Sone, N. Fukuzawa, and H. Zaha for their kind arrangement for breeding AhR-null mice. The authors also thank Dr H Nishimura for useful discussions and C. Yokoi, Y. Takeuchi, K. Taki, and Z. Sultana for their excellent technical assistance. The project was supported in part by a Core Research for Evolutionary Science and Technology grant from Japan Science and Technology Corporation (to C.T.).

References

Andreola F, Fernandez-Salguero PM, Chiantore MV, Petkovich MP, Gonzalez FJ, De Luca LM (1997) Aryl hydrocarbon receptor knockout mice (AHR /) exhibit liver retinoid accumulation and reduced retinoic acid metabolism. Cancer Res 57:2835–2838

Andreola F, Hayhurst GP, Luo G, Ferguson SS, Gonzalez FJ, Goldstein JA, De Luca LM (2004) Mouse liver CYP2C39 is a novel retinoic acid 4-hydroxylase. Its down-regulation o ers a molecular basis for liver retinoid accumulation and fibrosis in aryl hydrocarbon receptor-null mice. J Biol Chem 279:3434–3438

Bank PA, Salyers KL, Zile MH (1989) E ect of tetrachlorodibenzo-*p*-dioxin (TCDD) on the glucuronidation of retinoic acid in the rat. Biochim Biophys Acta 993:1–6

Brouwer A, Hakansson H, Kukler A, Van den Berg KJ, Ahlborg UG (1989) Marked alterations in retinoid homeostasis of Sprague–Dawley rats induced by a single i.p. dose of 10 micrograms/kg of 2,3,7,8-tetrachlorodibenzo-*p*-dioxin. Toxicology 58:267–283

Brucker-Davis F (1998) E ects of environmental synthetic chemicals on thyroid function. Thyroid 8:827–856

Chen LC, Berberian I, Koch B, Mercier M, Azais-Braesco V, Glauert HP, Chow CK, Robertson LW (1992) Polychlorinated and polybrominated biphenyl congeners and retinoid levels in rat tissues: structure–activity relationships. Toxicol Appl Pharmacol 114:47–55

Chin WW, Yen PM (1997) Molecular mechanisms of nuclear thyroid hormone action. In: Braverman LE (ed) Contemporary endoclinology: diseases of the thyroid. Humana Press, Totowa, NJ, pp 1–10

Elizondo G, Corchero J, Sterneck E, Gonzalez FJ (2000) Feedback inhibition of the retinaldehyde dehydrogenase gene ALDH1 by retinoic acid through retinoic acid receptor alpha and CCAAT/enhancer-binding protein beta. J Biol Chem 275:39747–39753

Emi Y, Ikushiro S, Iyanagi T (1996) Xenobiotic responsive element-mediated transcriptional activation in the UDP-glucuronosyltransferase family 1 gene complex. J Biol Chem 271:3952–3958

Fernandez-Salguero PM, Hilbert DM, Rudiko S, Ward JM, Gonzalez FJ (1996) Aryl-hydrocarbon receptor-deficient mice are resistant to 2,3,7,8-tetrachlorodibenzo-*p*-dioxin-induced toxicity. Toxicol Appl Pharmacol 140:173–179

Fletcher N, Hanberg A, Hakansson H (2001) Hepatic vitamin A depletion is a sensitive marker of 2,3,7,8-tetrachlorodibenzo-*p*-dioxin (TCDD) exposure in four rodent species. Toxicol Sci 62:166–175

Gonzalez FJ, Fernandez-Salguero P (1998) The aryl hydrocarbon receptor: studies using the AHR-null mice. Drug Metab Dispos 26:1194–1198

Got L, Gousson T, Delacoux E (1995) Simultaneous determination of retinyl esters and retinol in human livers by reversed-phase high-performance liquid chromatography. J Chromatogr B 668:233–239

Innami S, Nakamura A, Nagayama S (1974) Polychlorobiphenyl toxicity and nutrition. II. PCB toxicity and vitamin A (2). J Nutr Sci Vitaminol (Tokyo) 20:363–370

Kelly SK, Nilsson CB, Green MH, Green JB, Hakansson H (1998) Use of model- based compartmental analysis to study e ects of 2,3,7,8-tetrachlorodibenzo-*p*-dioxin on vitamin A kinetics in rats. Toxicol Sci 44:1–13

Koopman-Esseboom C, Morse DC, Weisglas-Kuperus N, Lutkeschipholt IJ, Van der Paauw CG, Tuinstra LG, Brouwer A, Sauer PJ (1994) E ects of dioxins and polychlorinated biphenyls on thyroid hormone status of pregnant women and their infants. Pediatr Res 36:468–473

Koopman-Esseboom C, Weisglas-Kuperus N, de Ridder MA, Van der Paauw CG, Tuinstra LG, Sauer PJ (1996) E ects of polychlorinated biphenyl/dioxin exposure and feeding type on infants' mental and psychomotor development. Pediatrics 97:700–706

Maden M, Gale E, Zile M (1998) The role of vitamin A in the development of the central nervous system. J Nutr 128:471S–475S

Mimura J, Yamashita K, Nakamura K, Morita M, Takagi TN, Nakao K, Ema M, Sogawa K, Yasuda M, Katsuki M, Fujii-Kuriyama Y (1997) Loss of teratogenic response to 2,3,7,8-tetrachlorodibenzo-*p*-dioxin (TCDD) in mice lacking the Ah (dioxin) receptor. Genes Cells 2:645–654

Munzel PA, Lehmkoster T, Bruck M, Ritter JK, Bock KW (1998) Aryl hydrocarbon receptor-inducible or constitutive expression of human UDP glucuronosyltransferase UGT1A6. Arch Biochem Biophys 350:72–78

Nilsson CB, Hakansson H (2002) The retinoid signaling system—a target in dioxin toxicity. Crit Rev Toxicol 32:211–232

Nilsson CB, Hoegberg P, Trossvik C, Azais-Braesco V, Blaner WS, Fex G, Harrison EH, Nau H, Schmidt CK, van Bennekum AM, Hakansson H (2000) 2,3,7,8-Tetrachlorodibenzo-*p*-dioxin increases serum and kidney retinoic acid levels and kidney retinol esterification in the rat. Toxicol Appl Pharmacol 169:121–131

Nishimura N, Miyabara Y, Sato M, Yonemoto J, Tohyama C (2002) Immunohistochemical localization of thyroid stimulating hormone induced by a low oral dose of 2,3,7,8-tetrachlorodibenzo-*p*-dioxin in female Sprague–Dawley rats. Toxicology 171:73–82

Nishimura N, Reeve VE, Nishimura H, Satoh M, Tohyama C (2000) Cutaneous metallothionein induction by ultraviolet B irradiation in interleukin-6 null mice. J Invest Dermatol 114:343–348

Nishimura N, Yonemoto J, Miyabara Y, Sato M, Tohyama C (2003) Rat thyroid hyperplasia induced by gestational and lactational exposure to 2,3,7,8-tetrachlorodibenzo-*p*-dioxin. Endocrinology 144:2075–2083

Peters JM, Narotsky MG, Elizondo G, Fernandez-Salguero PM, Gonzalez FJ, Abbott BD (1999) Amelioration of TCDD-induced teratogenesis in aryl hydrocarbon receptor (AhR)-null mice. Toxicol Sci 47:86–92

Ritter JK (2000) Roles of glucuronidation and UDP-glucuronosyltransferases in xenobiotic bioactivation reactions. Chem Biol Interact 129 171–193

Santostefano MJ, Richardson VM, Walker NJ, Blanton J, Lindros KO, Lucier GW, Alcasey SK, Birnbaum LS (1999) Dose-dependent localization of TCDD in isolated centrilobular and periportal hepatocytes. Toxicol Sci 52:9–19

Sass JO, Tzimas G, Nau H (1994) 9-*cis*-Retinoyl-beta-D-glucuronide is a major metabolite of 9-*cis*-retinoic acid. Life Sci 54:PL69–PL74

Schmidt CK, Hoegberg P, Fletcher N, Nilsson CB, Trossvik C, Hakansson H, Nau H (2003) 2,3,7,8-tetrachlorodibenzo-*p*-dioxin (TCDD) alters the endogenous metabolism of all-*trans*-retinoic acid in the rat. Arch Toxicol 77:371–383

Schrader M, Carlberg C (1994) Thyroid hormone and retinoic acid receptors form heterodimers with retinoid X receptors on direct repeats, palindromes, and inverted palindromes. DNA Cell Biol 13:333–341

Tritscher AM, Goldstein JA, Portier CJ, McCoy Z, Clark GC, Lucier GW (1992) Dose–response relationships for chronic exposure to 2,3,7,8-tetrachlorodibenzo-*p*-dioxin in a rat tumor promotion model: quantification and immunolocalization of CYP1A1 and CYP1A2 in the liver. Cancer Res 52:3436–3442

Umesh CG, Shobhita C (1999) The status of retinoids in women su ering from hyper- and hypothyroidism: interrelationship between vitamin A, β-carotene and thyroid hormones. Int J Vit Nutr Res 69:123–135

Vreugdenhil HJ, Slijper FM, Mulder PG, Weisglas-Kuperus N (2002) E ects of perinatal exposure to PCBs and dioxins on play behavior in Dutch children at school age. Environ Health Perspect 110:A593–A598

Zile MH, Inhorn RC, DeLuca HF (1982) Metabolites of all-trans-retinoic acid in bile: identification of all-*trans*- and 13-*cis*-retinoyl glucuronides. J Biol Chem 257:3537–3543

Zile MH, Schnoes HK, DeLuca HF (1980) Characterization of retinoyl beta-glucuronide as a minor metabolite of retinoic acid in bile. Proc Natl Acad Sci USA 77:3230–3233

Constitutively Active Aryl Hydrocarbon Receptor Expressed Specifically in T-Lineage Cells Causes Thymus Involution and Suppresses the Immunization-Induced Increase in Splenocytes[1]

Keiko Nohara,[2]* Xiaoqing Pan,* Shin-ichi Tsukumo,* Azumi Hida,† Tomohiro Ito,* Haruko Nagai,*‡ Kaoru Inouye,* Hozumi Motohashi,† Masayuki Yamamoto,† Yoshiaki Fujii-Kuriyama,† and Chiharu Tohyama*

The aryl hydrocarbon receptor (AhR) is a transcription factor belonging to the basic helix-loop-helix-PER-ARNT-SIM superfamily. Xenobiotics, such as 2,3,7,8-tetrachlorodibenzo-*p*-dioxin, bind the receptor and trigger diverse biological reactions. Thymocyte development and T cell-dependent immune reactions are sensitive targets of AhR-dependent 2,3,7,8-tetrachlorodibenzo-*p*-dioxin toxicity. However, the exact role of the AhR in T cells in animals exposed to exogenous ligands has not been clarified because indirect effects of activated AhR in other cell types cannot be excluded. In this study, we generated transgenic (Tg) mice expressing a constitutively active mutant of AhR under the regulation of a T cell-specific CD2 promoter to examine AhR function in T cells. The mRNAs of the constitutively active mutant of AhR and an AhR-induced gene, CYP1A1, were expressed in the thymus and spleen of the Tg mice. The transgene expression was clearly detected in the thymocytes, CD4, and CD8 T cells, but not in the B cells or thymus stromal cells. These Tg mice had a decreased number of thymocytes and an increased percentage of CD8 single-positive thymocytes, but their splenocytes were much less affected. By contrast, the increase in number of T cells and B cells taking place in the spleen after immunization was significantly suppressed in the Tg mice. These results clearly show that AhR activation in the T-lineage cells is directly involved in thymocyte loss and skewed differentiation. They also indicate that AhR activation in T cells and not in B cells suppresses the immunization-induced increase in both T cells and B cells. ***The Journal of Immunology*****, 2005, 174: 2770–2777.**

Xenobiotics, such as polycyclic aromatic hydrocarbons and halogenated aromatic hydrocarbons, bind and activate the aryl hydrocarbon receptor (AhR),[3] a transcription factor belonging to the basic helix-loop-helix-PER-ARNT-SIM (bHLH-PAS) superfamily (1, 2), and elicit diverse biological and physiological responses (3–6). These findings suggest that the AhR functions physiologically as a ligand-dependent transcription factor, whereas the endogenous ligands and intrinsic role of the AhR have yet to be identified. The decreased fertility and abnormalities found in various organs, including the liver, spleen, vascular structures, ovary, mammary gland, and bone marrow lymphocytes, in AhR-deficient mice (7–12) also imply intrinsic roles of the AhR in normal developmental processes. In the absence of ligands, the AhR exists in the cytoplasm in an inactivated form complexed with a dimer of heat shock protein 90 and the immunophilin homologue hepatitis B virus X-associated protein 2 (13). Upon binding with ligands, such as its most potent ligand, 2,3,7,8-tetrachlorodibenzo-*p*-dioxin (TCDD), the AhR becomes activated, dissociates from the protein complex, and translocates into the nucleus, where the receptor dimerizes with another basic helix-loop-helix-PAS transcription factor, aryl hydrocarbon receptor nuclear translocator (ARNT). The AhR/ARNT heterodimer specifically binds DNA sequences, called xenobiotic responsive elements (XREs), distributed in the enhancer regions of various genes, including one of the most sensitive targets, CYP1A1, and modulates their expression (14). The receptor complex also interacts with various nuclear proteins, such as retinoblastoma, NF-κB, and estrogen receptors (15–17). However, determination of the functions of the AhR requires identification of the genes and proteins that it modulates and the cell types in which the individual biological or physiological reactions occur.

The immune system is one of the sensitive targets of TCDD (6). Although a major portion of TCDD toxicities, such as thymus involution, suppressed CTL activity, and reduced Ab production, have been demonstrated to be mediated through the AhR by studies in AhR-deficient mice (18–20), the precise mechanisms of AhR function, including the primary cellular targets and biological reactions involved in these toxic effects, remain to be clarified. The thymus involution induced by administration of TCDD or other AhR ligands to mice is characterized by decreases in tissue weight and cell number that are mainly attributable to a decrease in $CD4^+CD8^+$ double-positive (DP) cells, the predominant population of thymocytes. Skewing of thymocyte differentiation toward CD8 single-positive (SP) T cells is another peculiar feature of the

*Environmental Health Sciences Division, National Institute for Environmental Studies and †Center for Tsukuba Advanced Research Alliance, University of Tsukuba, Tsukuba, Japan; and ‡Research Institute for Biological Sciences, Science University of Tokyo, Noda, Japan

Received for publication August 10, 2004. Accepted for publication December 20, 2004.

The costs of publication of this article were defrayed in part by the payment of page charges. This article must therefore be hereby marked *advertisement* in accordance with 18 U.S.C. Section 1734 solely to indicate this fact.

[1] K.I. was supported by the Japan Society for the Promotion of Science (Domestic Research Fellowship).

[2] Address correspondence and reprint requests to Dr. Keiko Nohara, Environmental Health Sciences Division, National Institute for Environmental Studies, Tsukuba 305-8506, Japan. E-mail address: keikon@nies.go.jp

[3] Abbreviations used in this paper: AhR, aryl hydrocarbon receptor; PAS, PER-ARNT-SIM; TCDD, 2,3,7,8-tetrachlorodibenzo-*p*-dioxin; ARNT, aryl hydrocarbon receptor nuclear translocator; XRE, xenobiotic responsive element; DP, double-positive; SP, single-positive; FTOC, fetal thymus organ culture; Tg, transgenic; CA-AhR, constitutively active mutant of AhR; h, human; DIG, digoxigenin; 7-AAMD, 7-aminoactinomycin D; DN, double negative.

0022-1767/05/$02.00

response to TCDD exposure (18, 21, 22). All of these features are reproduced in vitro by direct addition of TCDD to fetal thymus organ culture (FTOC) (19, 23, 24), indicating that the target cells responsible for the alterations are present in the thymus. The results of previous studies that have included histological examination have led to the hypothesis that thymic stromal cells, and not thymocytes themselves, are the direct targets of TCDD that induce thymus involution (25). This hypothesis was supported by a study showing that the stroma of a fetal thymus reaggregation culture treated with an AhR-binding halogenated aromatic hydrocarbon, not the thymocytes, induced thymus involution (24). By contrast, a recent study in which chimeric mice having AhR-deficient hemopoietic cells and wild-type stromal cells or vice versa were exposed to TCDD demonstrated that the AhR in the hemopoietic compartment, that is in the thymocytes or their precursor cells, is responsible for the TCDD-induced thymus involution (18).

The results of other studies have also shown or suggested that the AhR in T cells plays an essential role in TCDD-induced immunotoxicity. A recent study by Kerkvliet et al. (26) in a mouse graft-vs-host model injected with $AhR^{+/+}$ or $AhR^{-/-}$ T cells showed that AhR activation in T cells is critical to the suppression of CTL activity by TCDD. In our own study examining the effect of TCDD on OVA-specific Ab production in mice (27), TCDD exposure suppressed the increase in T cell number in the spleen and production of IL-2 and Th2-type cytokines before the inhibition of Ag-induced Ab production, suggesting that the AhR activation in T cells causes suppression of T cell activation and subsequent immune reactions leading to Ab production. However, it is difficult to determine the specific role of AhR activation in T cells alone in TCDD-exposed mice, because the AhR in all cell types, including B cells and APCs, is simultaneously activated, and indirect effects cannot be excluded. Chimeric mouse models and a T cell transfer system produced by using AhR-deficient mice or their cells are very useful tools for studying the primary cell target of TCDD, but they are inconvenient, because generation of chimeric mice and reconstitution by T cell transfer require highly specialized techniques. In addition, when chimeric mice are used, it must be borne in mind that their hemopoietic cells contain precursor cells not only for T cells but for B cells and APCs as well (28).

To investigate the role of AhR activation in TCDD-induced immunotoxicity, in the present study we generated transgenic (Tg) mice that specifically express a constitutively active mutant of AhR (CA-AhR) in T-lineage cells by expressing a CA-AhR with a minimal deletion in the PAS-B domain (29) under the regulation of a CD2 promoter. The AhR mutant constitutively localizes to the nucleus, heterodimerizes with ARNT, and activates transcription by binding XRE sequences in a ligand-independent manner (29, 30). The results of the present study demonstrate that AhR activation in T-lineage cells alone directly induces the thymocyte changes. They also show that the increase in number of splenocytes after immunization is suppressed in the Tg mice, whereas resting splenocytes in nonimmunized mice are much less affected, suggesting that the AhR plays a role in the growth of activated and proliferating T cells.

Materials and Methods

Generation of Tg mice

The CA-AhR expression construct (VA hCD2-CA-AhR) was generated by subcloning PAS B-domain-deleted mouse AhR cDNA with poly(A) signal (29) into the *EcoRI/BamHI* site of the VA human CD2 (hCD2) minigene, an improved version of a human CD2 minigene-based vector (31). Tg founder mice were obtained by microinjecting the transgene expression construct into C57BL/6J × DBA/2 eggs as described previously (32). In some lines, VA hCD2-GFP was coinjected with VA hCD2-CA-AhR. One line carrying both CA-AhR and GFP constructs (line A) and two lines with the CA-AhR construct alone (lines K and N) were chosen for further studies and subsequently were backcrossed into C57BL/6J mice. Founders and subsequent littermates were genotyped by PCR of tail DNA using primers for VA hCD2-CA-AhR (5′-GAACAGAGAGTTTGTCCAGC-3′, located in hCD2 promoter, and 5′-CTTCCAAAGGTAAGCATAAGAGTC-3′, located in N terminus of CA-AhR). Integrated CA-AhR copy number was determined by Southern blot analysis. Genomic DNA from a tail sample was digested with *Eco*RI and *Pst*I, separated by agarose gel electrophoresis, blotted onto a Hybond filter (Amersham), and hybridized with a digoxigenin (DIG)-labeled probe. The DIG-labeled probe was synthesized from the *Hinc*II digestion fragment of pEB6CAG-CA-AhR-GFP (29) with a DIG-high prime DNA labeling and detection starter kit I (Roche Diagnostics) and was detected with CSPD as a substrate according to the manufacturer's instructions. Heterozygous ($CA\text{-}AhR^{+/-}$) mice were used for experiments after crossing into C57BL/6 mice for two to six generations. Their nontransgenic ($CA\text{-}AhR^{-/-}$) littermates (designated as wild type) were used as controls.

Cell preparation

Single cell suspensions of thymus and spleen were prepared by forcing cells in RPMI 1640 medium supplemented with 12 mM HEPES (pH 7.1), 0.05 mM 2-ME, 100 U/ml penicillin, 100 μg/ml streptomycin, and 10% FCS (complete medium) through a stainless-steel mesh. Spleen cells and bone marrow cells prepared from thigh bones were treated with ammonium chroride/EDTA solution (0.83% NH_4Cl, 0.1% $KHCO_3$, 0.37% EDTA (pH 7.4)) for 2 min at room temperature to eliminate RBCs and then were washed with PBS (33). Cells were counted with a hemocytometer after staining with trypan blue.

RT-PCR

Total RNA was isolated from cells or tissues with an RNeasy Mini kit (Qiagen). After checking the quality of the RNA by electrophoresis, RT-PCR was performed with an RNA LA PCR kit (AMV) ver1.1 (TaKaRa Biomedicals) according to the manufacturer's instructions. The amplification was conducted by heating at 94°C for 2 min, cycling at 94°C for 30 s, 60 or 66°C for 30 s, and 72°C for 30 s, and then extension at 72°C for 10 min after the final cycle. The primer sequences and annealing temperatures for each gene are shown in Table I. The primers for detecting mRNA expression of CA-AhR were designed to span the region coding for PAS B domain to distinguish PCR products between CA-AhR and wild-type AhR. The PCR products were separated with a 1.2% Synergel (Diversified Biotech) containing 0.5 μg/ml ethidium bromide, and the gel images were captured and visualized using an Electrophoresis Documentation and Analysis System 290 (Eastman Kodak).

Flow cytometry

Cells were stained with mAbs against lymphocyte surface markers or streptavidin-allophycocyanin (BD Pharmingen) for 20 min on ice. After staining, the cells were washed, treated with 7-aminoactinomycin D (7-AAMD; Sigma-Aldrich) to label dead cells, and measured with a FACSCalibur (BD Biosciences). Live cells were gated and analyzed (22). The following mAbs, all purchased from BD Pharmingen, were used: PE-conjugated anti-CD4 (anti-CD4-PE, clone GK-1.5), FITC-conjugated anti-CD8

Table I. *List of primers used for RT-PCR*

Description	Primer Sequence (5′-3′)	Annealing Temperature (°C)	Product Size (bp)
CA-AhR	TTACCTGGGCTTTCAGCAGT	66	506
	AACTGGGGTGGAAAGAATCC		
CYP1A1	CCATGACCGGGAACTGTGG	60	344
	TCTGGTGAGCATCCTGGACA		
Adseverin	GTGCTTCTAAGCATTTCCCC	60	121
	GAGTGAATGGCATCCAAGTG		
CD4	AAGGGCTCTCCCTGAGAGTC	60	104
	AAAGAGGAAAAAAGGGGAAGG		
Spatial	GAAGGTGACAGCGAAAATCA	60	112
	AAGGCATTAGACAGGTTGGG		
β-Actin	GAGGCCCAGAGCAAGAGAG	60	225
	GGCTGGGGTGTTGAAGGT		
HPRT	GCTGGTGAAAAGGACCTCT	60	249
	CACAGGACTAGAACACCTGC		

(anti-CD8-FITC, clone 53-6.7), biotinylated anti-CD8 (anti-CD8-biotin, clone 53-6.7), anti-CD3-PE (clone 145-2C11), anti-CD19-biotin (clone ID3), anti-B220-FITC (clone RA3-6B2), anti-CD127(IL-7Rα)-biotin (clone B12-1), and anti-CD61-PE (clone 2C9.G3). Biotinylated rat IgG2a was used as an isotype-matched control.

Immunization

OVA (albumin, chicken egg, grade VII) was purchased from Sigma-Aldrich. Alum-precipitated OVA (OVA/alum) was prepared as follows (27, 34). OVA (1 mg/ml) in PBS was mixed with an equal volume of 9% (w/v) $AlK(SO_4)_2$, and pH of the mixture was adjusted to 6.5 with KOH. The precipitate was washed three times with PBS and then resuspended in PBS at 0.5 mg/ml. Mice were i.p. immunized with the OVA/alum (100 μg OVA/mouse).

TCDD treatment

TCDD (50 μg/ml in nonane) purchased from Cambridge Isotope Laboratories was diluted with corn oil to adjust it to a dose volume of 10 μl/g body weight. TCDD was administered to the mice orally.

Fetal thymus organ culture

Line A heterozygous Tg mice backcrossed into C57BL/6J mice for five generations were mated, and homozygous CA-AhR$^{+/+}$ Tg mice were obtained. Male CA-AhR$^{+/+}$ mice were mated with female C57BL/6J mice, and thymuses were collected from fetuses on gestation day 16.5. One or two lobes of the thymuses were placed on a nitrocellulose filter (45-μm pore size) set in a 24-well culture plate with 1 ml of complete medium and were cultured for 4 days (35). To deplete them of thymocytes, the lobes were cultured in the presence of 1.35 mM 2-deoxyguanosine (Sigma-Aldrich) for 4 days (36, 37).

Results

Generation of T cell-specific CA-AhR Tg mice

We used the VA hCD2 vector to generate Tg mice expressing a CA-AhR mutant (Fig. 1*A*) specifically in T-lineage cells. We chose one line carrying both CA-AhR and GFP constructs (line A) and two lines with only the CA-AhR construct (lines K and N) functioning under the control of the VA hCD2 vector for the subsequent experiments. The transgene-positive mice were mated with C57BL/6 mice and maintained as heterozygotes. Heterozygous mice were used in all experiments unless otherwise specified, and their nontransgenic (CA-AhR$^{-/-}$) littermates (designated as wild type) were used as controls. Integrated CA-AhR copy numbers were determined by Southern blotting to be 2 for line A, 6–7 for line K, and 9–11 for line N. All of the lines were fertile, exhibited a normal sex ratio at birth, showed no increase in mortality after birth, and appeared healthy.

Fig. 1*B* shows CA-AhR mRNA expression in various organs in line A Tg mice. CA-AhR mRNA was detected in the thymus and spleen as expected, and was also found in the lung and, to a very minor extent, in the kidney. Expression of the AhR-responsive gene CYP1A1 was also detected in the thymus and spleen in the Tg mice in contrast with their wild-type littermate mice (Fig. 1*C*). In the lung, CYP1A1 mRNA was detected in the wild-type mice. The lung is reported to express the highest level of AhR mRNA among the tissues examined, including the thymus and spleen, in the mice (38). Recently, endogenous ligand was isolated from porcine lung (39). Thus, the lung may contain abundant AhR and endogenous ligand may activate the receptor and induce CYP1A1. The expression of CYP1A1 in the lung was further increased in the Tg mice (Fig. 1*C*). Expression of CA-AhR and CYP1A1 mRNA was also confirmed in the thymus and spleen of lines K and N (see Fig. 4).

Expression of the transgene in immune cells was measured by flow cytometry analysis of the GFP expression in line A Tg mice (Fig. 2). Thymocytes showed a broader peak of the GFP-positive population (Fig. 2*A*). CD4 and CD8 T cells in the spleen were confirmed to be GFP-positive, and B cells did not express GFP (Fig. 2*B*).

We then investigated whether the bone marrow cells of the CA-AhR Tg mice expressed the transgene and, as shown in Fig. 3, the CD3$^-$CD127$^+$ (IL-7Rα-expressing) lymphocyte progenitor fraction (40) was found to be faintly GFP-positive (Fig. 3*C*, R3). Although a previous study reported that the VA hCD2 vector functions in megakaryocytes as well as T-lineage cells (32), CD61$^+$ megakaryocytes (41) in the bone marrow did not express the transgene (Fig. 3*C*, R4 and R5).

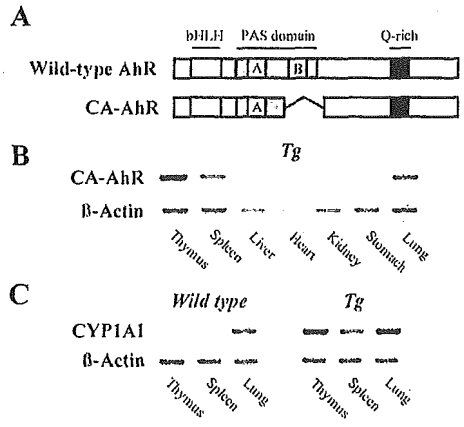

FIGURE 1. Generation of T cell-specific CA-AhR Tg mice. *A*, Schematic representation of the wild-type mouse AhR and the CA-AhR mutant lacking the minimal PAS B motif. *B*, Different tissues from line A heterozygous Tg mice were examined for CA-AhR mRNA expression by RT-PCR. C, Functional activation of the CA-AhR was confirmed by detection of CYP1A1 expression by RT-PCR.

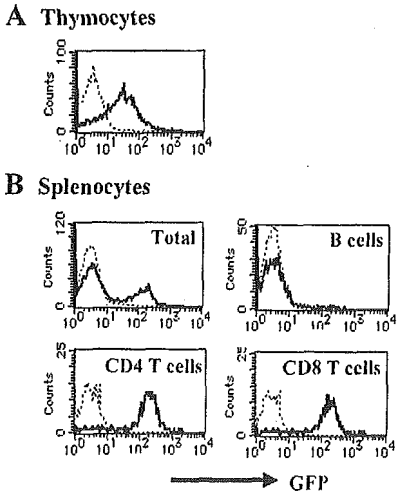

FIGURE 2. Transgene expression in thymocytes and splenocytes. *A*, Thymocytes prepared from line A heterozygous mice were stained with 7-AAMD and analyzed with a FACSCalibur flow cytometer. 7-AAMD-negative live cells were gated and expression of coinjected GFP was analyzed. *B*, Splenocytes from line A heterozygous mice were stained with a combination of anti-CD19-biotin/streptavidin-allophycocyanin and anti-CD3-PE or a combination of anti-CD8-biotin/streptavidin-allophycocyanin and anti-CD4-PE and then were stained with 7-AAMD and analyzed with a FACSCalibur. CD4 T cells, CD8 T cells, and CD19$^+$ B cells in the 7AAMD-negative live cells were gated, and GFP expression was analyzed. The staining obtained in Tg mice is represented by the bold line, and the staining in wild-type mice is represented by the dotted line.

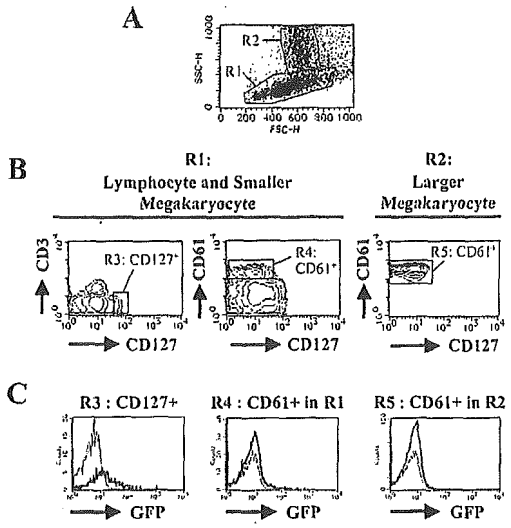

FIGURE 3. The transgene is faintly expressed in CD127$^+$ cells in the bone marrow. Bone marrow cells from line A heterozygous mice were stained with anti-CD127-biotin/streptavidin-allophycocyanin and either anti-CD3-PE or anti-CD61-PE and then were stained with 7-AAMD and analyzed with a FACSCalibur. *A*, Side scatter vs forward scatter of the cells analyzed. Region 1 (R1), including lymphocytes and smaller size megakaryocyte, and R2, including larger size megakaryocytes (41), in the 7-AAMD-negative live cells are indicated in the dot plot. *B*, R3, including CD127$^+$ cells, and R4, including CD61$^+$ cells in R1, and R5, including CD61$^+$ cells in R2, are indicated in the contour plot. *C*, Expression of GFP as analyzed by gating R3–R5 is shown in the histogram plot. The staining obtained in Tg mice is represented by the bold line, and the staining in wild-type mice is represented by the thin line.

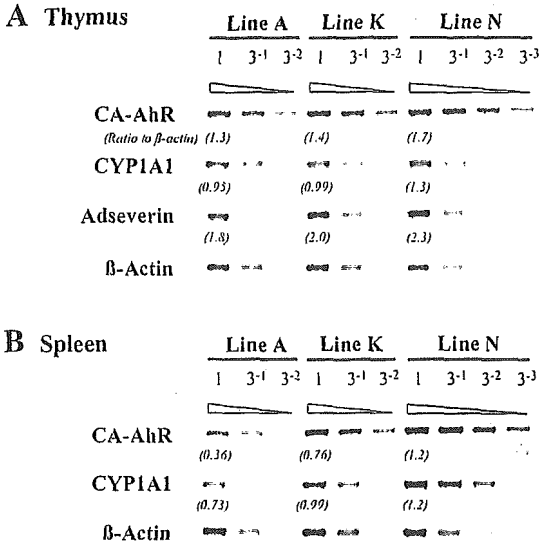

FIGURE 4. Comparison of CA-AhR and target gene expression in the thymus and spleen from line A, line K, and line N heterozygous mice. Total RNA was prepared from the thymus and spleen of the three lines with the RNeasy mini kit. cDNAs prepared from 20 ng of total RNA and serial dilutions (3^{-1}–3^{-3}) were amplified by PCR using primers for CA-AhR, CYP1A1, adseverin, or β-actin as a housekeeping gene. The expression of genes was quantified by densitometrically scanning gel images, and the values normalized to β-actin mRNA are indicated in parentheses. The numbers of PCR cycles for CA-AhR in thymus and spleen were 32 and 34, respectively, 26 and 32 for CYP1A1, and 20 for β-actin in both tissues. Mice were used after crossing into C57BL/6 mice for six generations in line A and for three generations in lines K and N.

CA-AhR expression induces target gene mRNA in both thymus and spleen, but reduces thymocyte number alone

Expression of the CA-AhR transgene and its target genes and phenotypic changes in the thymus and spleen were examined in the three lines. RT-PCR analyses showed that CA-AhR and CYP1A1 expression in the thymuses and spleens of lines A, K, and N were increased according to the integrated CA-AhR gene numbers (Fig. 4). Expression of adseverin, which was reported to be induced by TCDD in mice thymuses in an AhR-dependent manner (37), was also increased according to the transgene numbers.

The thymus weight was reduced in all three lines, by 36% in line A, 70% in line K, and 63% in line N (Fig. 5*A*). The thymocyte number was reduced by 49% in line A, 96% in line K, and 92% in line N (Fig. 5*A*). The thymocyte population defined by CD4 and CD8 expression was also affected in the Tg mice, with reduced percentages of CD4$^+$CD8$^+$ DP cells and increased percentages of CD8 SP and double negative (DN) cells (Table II). The ratios of CD4 SP/CD8 SP were significantly reduced in the Tg mice (Table II). The remarkable increases in the percentage of DN cells in line K and N were parallel to the large decreases in the total cell numbers.

By contrast, spleen weight was unaffected by the expression of CA-AhR (Fig. 5*B*). Splenocyte number was significantly reduced only in line N (by 40%), in which CA-AhR is most highly expressed (Fig. 5*B*), and the percentages of CD4 T cells, CD8 T cells, and B cells were unchanged, even in line N (data not shown). All of these findings are consistent with those observed in the thymuses exposed to TCDD (18, 21, 22).

We further confirmed that the CA-AhR is not expressed in the stromal cells and that CA-AhR expression in T-lineage cells alone is capable of inducing the thymus alteration in FTOC. mRNA expression was examined in whole thymus and stroma obtained by culturing thymus tissues in the presence of 2-deoxyguanosine to deplete it of thymocytes. As expected, CD4 mRNA was detected only in whole thymus, and Spatial mRNA, which is specifically expressed in thymic stromal cells (42), was detected in both the

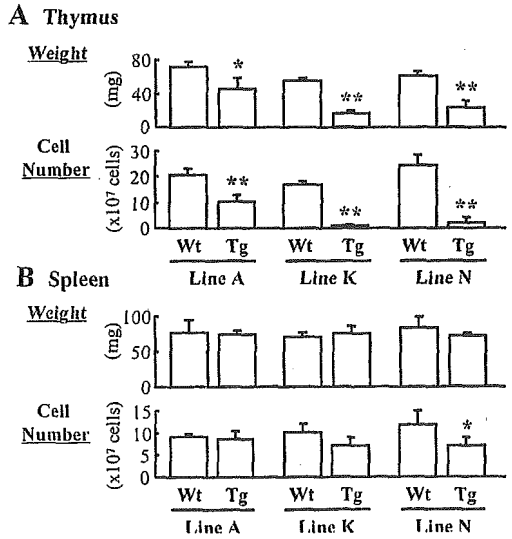

FIGURE 5. CA-AhR expression in T-lineage cells reduces thymus weight and cell number, but affects the spleen less. Thymus and spleen from female heterozygous Tg mice and nontransgenic littermate wild-type mice of line A (8 wk old, n = 4/each group), line K (10 wk old, n = 5), and line N (8–9 wk old, n = 5) were examined. Mice were used after crossing into C57BL/6 mice for two generations in line A and for three generations in lines K and N. The differences between Tg mice and wild-type mice were analyzed by Student's t test. The data are expressed as mean ± SD. *, $p < 0.05$; **, $p < 0.01$.